Accepted Manuscript

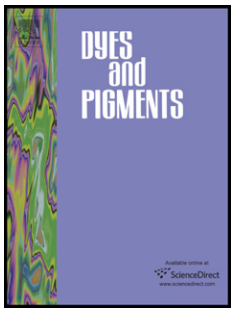

Sterically demanded unsymmetrical zinc phthalocyanines for dye-sensitized solar cells

L. Giribabu, V.K. Singh, Tejaswi Jella, Y. Soujanya, Anna Amat, Filippo De Angelis, Aswani Yella, Peng Gao, Mohammad Khaja Nazeeruddin

PII: S0143-7208(13)00134-4

DOI: 10.1016/j.dyepig.2013.04.007

Reference: DYPI 3906

To appear in: *Dyes and Pigments*

Received Date: 12 December 2012

Revised Date: 1 April 2013

Accepted Date: 5 April 2013

Please cite this article as: Giribabu L, Singh VK, Jella T, Soujanya Y, Amat A, De Angelis F, Yella A, Gao P, Nazeeruddin MK, Sterically demanded unsymmetrical zinc phthalocyanines for dye-sensitized solar cells, *Dyes and Pigments* (2013), doi: 10.1016/j.dyepig.2013.04.007.

Sterically Demanded Unsymmetrical Zinc Phthalocyanines for Dye-Sensitized Solar Cells

L. Giribabu, V.K. Singh, T. Jella, Y. Soujanya, Anna Amat, Filippo De Angelis, Aswani Yella, Peng Gao, Mohammad Khaja Nazeeruddin

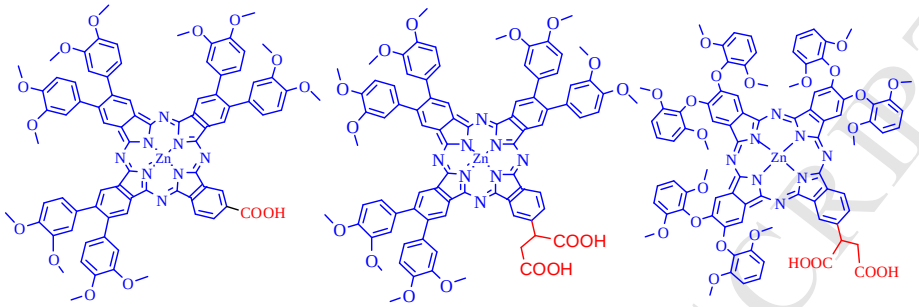

DMPCH-1 **DMPCH-2** **DMPCH-3**

Three new sterically demanded unsymmetrical zinc phthalocyanines have been designed, synthesized and characterized for dye-sensitized solar cell applications.

Sterically demanded unsymmetrical zinc phthalocyanines for dye-sensitized solar cells

L. Giribabu,[a*] V.K. Singh,[a] Tejaswi Jella,[a] Y. Soujanya,[b] Anna Amat,[c,d] Filippo De Angelis,[c] Aswani Yella,[e] Peng Gao,[e] Mohammad Khaja Nazeeruddin[e]

[a]*Inorganic & Physical Chemistry Division, CSIR-Indian Institute of Chemical Technology, Hyderabad-500607, India.* Tel.: +91-40-27191724; fax: +91-40-27160921; e-mail: giribabu@iict.res.in

[b]*Molecular Modelling Group, CSIR-Indian Institute of Chemical Technology, Hyderabad-500067, Indi*

[c]*Computational Laboratory for Hybrid/Organic Photovoltaics (CLHYO), Istituto CNR di Scienze Tecnologie Molecolari, Via Elce di Sotto 8, I-06123, Perugia, Italy*

[d]*Dipartimento di Chimica, Università di Perugia, Via elce di Sotto 8, 06213 Perugia, Italy*

[e]*Laboratory for Photonics and Interfaces, Institute of Chemical Sciences and Engineering, School of basic Sciences, Swiss Federal Institute of Technology, CH - 1015 Lausanne, Switzerland.*

ABSTRACT

Three new sterically demanding unsymmetrical zinc phthalocyanines have been designed and synthesized as sensitizers for dye-sensitized solar cells. All three unsymmetrical phthalocyanines have been completely characterized by elemental analyses, mass spectrometry, FT-IR, ^{1}H NMR, UV-Visible, and fluorescence (steady-state and life-time) spectroscopies as well as electrochemical methods. Photophysical properties (absorption, emission and redox properties) indicate that the LUMO of unsymmetrical phthalocyanines lies above the TiO_2 conduction band and HOMO is below the redox electrolyte. The experimental results are supported by DFT/TD-DFT studies. Electrochemical and *in-situ* spectroelectrochemical studies suggest that the redox reactions belong to the macrocyclic ring-based electron transfer processes. All three unsymmetrical phthalocyanines were tested in DSSC using I^-/I_3^- redox electrolyte system.

Keywords: Dye-Sensitized solar cells, Phthalocyanine, Unsymmetry, Absorption, Spectroelectrochemistry, Redox Electrolyte.

1. Introduction

The world is rapidly approaching a precarious environmental state owing to the extensive use of fossil fuels, which may be depleted in the near future. In this regard, solar energy is expected to play a key role in sustainable development [1]. Among the various photovoltaic technologies, dye-sensitized solar cells, (DSSC) have emerged alongside conventional *p-n* junction solar cells [2-4]. In a typical DSSC, upon photo excitation, the dye injects an electron into the conduction band of a nanocrystalline film of a wide-band-gap oxide semiconductor, such as titanium dioxide (TiO_2), and is subsequently regenerated back to the ground state by electron donation from a redox couple. Energy conversion efficiencies up to 11.4% have been achieved using Ru(II) polypyridyl complexes as molecular sensitizers [5-6]. However, Ru(II) polypyridyl complexes are expensive to the rarity of the metal in the earth's crust and also they lack strong absorption in the red or near-infrared region (NIR), where the solar flux of photons is still significant, thus limiting the realization of high efficient devices. For this reason, dyes with large π-conjugated systems such as porphyrins and phthalocyanines are receiving considerable attention for sensitization of nanocrystalline TiO_2 in view of their efficient electron transfer process [7-9]. Recently, Grätzel, Diau, and Yeh et al. have reported a DSSC with an incorporated porphyrin dye having a cell performance that achieves with an efficiency of 12.3% [10].

Phthalocyanine (Pc) derivatives are also suitable DSSC sensitizers because of their intense and tunable absorption in the red to NIR, transparency over a large portion of the visible spectrum, and extraordinary thermal as well as photochemical stability [11-12]. However, the efficiencies of DSSC employing phthalocyanines as sensitizers have not been impressive. This is mainly due to the fact that the phthalocyanine molecule has strong tendency to aggregate on the TiO_2 surface and also a lack of directionality of the electron transfer in the excited state. Nazeeruddin and co-workers reported an unsymmetrical amphiphilic zinc phthalocyanine (PCH001, *see* Figure 1) having three bulky *tert*-butyl groups, which minimizes the aggregation and two carboxylic acids in its molecular structure showing an overall conversion efficiency of up to 3.05% [13-14]. Moreover, Mori et al. recently confirmed that the presence of bulky substituents at peripheral positions of phthalocyanine macrocyle, completely suppress aggregation and, therefore achieved high energy conversion efficiency of 4.6% [15]. The carboxyl-functionalized zinc phthalocyanine substituted at the periphery with six 2,6-diphenylphenoxy groups achieved up to a 4.6 %

conversion efficiency. Recently, Torres and co-workers have extended this concept and introduced more rigid π-conjugated bridges (either C=C or C≡C bond) between the anchoring carboxyl groups and the phthalocyanine macrocycle with an overall conversion of up to 6.13% [16].

In this manuscript, as part of our efforts to investigate further improvement of efficiency of DSSC devices based on phthalocyanine sensitizers, we report the synthesis and photovoltaic characterizations of a series of sterically demanded phthalocyanines (**DMPCH-1**, **DMPCH-2** and **DMPCH-3**) shown in Figure 1. **DMPCH-1&2** differ in having number of anchoring groups and **DMPCH-3** possesses a different donor moiety. All the sensitizers have been completely characterized by elemental analyses, Mass, ^{1}H NMR, UV-Vis and emission spectroscopies (both steady-state and time-resolved), as well as cyclic voltammetry including spectroelectrochemistry. The studied phthalocyanines have also been investigated computationally by means of DFT and TDDFT theories. The introduction of 3,4-dimethoxy phenyl and 2,6-dimethoxy phenyl at the six peripheral positions of the benzene rings of phthalocyanine **DMPCH-1&2** and **DMPCH-3**, respectively, is supposed to cause steric crowding and hence reduce the aggregation, which will afford high power conversion. The structures of three unsymmetrical phthalocyanines are shown in Figure 1. We have used I^-/I_3^- based redox electrolyte for the fabrication of devices.

2. Experimental

4,5-dichlorophthalnitrile, 3,4-dimethoxyphenyl boronic acid, 2,6-dimethoxy phenol, 1,8-diazabicyclo[5.4.0]undec-7-ene, $Pd(PPh_3)_4$, K_3PO_4, and $Zn(OAc)_2$ are procured from Aldrich and were used as such. The solvents 1,4-dioxane, THF, 1-pentanol, and DMF were obtained from BDH (India) and were purified prior to use [17]. Analytical grade ethanol was also obtained from BDH and was used as such. Column chromatography was performed on Aceme silica gel (60-120).

2.1. Synthesis

3,4-dimethoxy phenyl boronic acid (**1**), 3,4-dicyanobenzoic acid (**3**) and triester phthalonitrile were synthesized as per the literature methods [18,19].

2.1.1. 4,5-Bis(3,4-dimethoxyphenyl) phthalonitrile (**2**):

Anhydrous 1,4-dioxane (20 mL) was taken in a 100 mL round bottom flask. To this charged with 4,5-dichlorophthalonitrile (0.32 g, 1.62 mmol), 3,4-dimethoxyphenyl boronic acid (1.0 g, 5.5 mmol), P(o-Tolyl)$_3$ (0.1 g, 0.323 mmol), K_3PO_4 (2.05 g, 9.70 mmol) and then flushed with nitrogen for 15 minutes before the addition of $Pd(PPh_3)_4$ (0.04 g, 0.032 mmol). The reaction mixture was stirred at 90 ^{0}C for 6 h under nitrogen atmosphere. After cooling to room temperature, the reaction mixture was washed twice with water. The combined organic layers were washed once with water, subsequently dried over anhydrous sodium sulphate, filtered and concentrated by rotary evaporator. The resultant solid material was subjected to silica gel column chromatography and eluted with hexane-ethyl acetate to obtain the desired product as yellow powder in 67% yield (0.44 g). FT-IR (KBr) υ_{max} 2928, 2223 (CN), 1254, 1024 cm^{-1}. ^{1}H NMR (300 MHz, $CDCl_3$): δ (ppm) 7.76 (s, 2H), 6.62-6.78 (m, 4H), 6.47 (s, 2H), 3.82 (s, 6H), 3.56 (s, 6H); EI-MS (m/z): $C_{24}H_{20}N_2O_4$ [400.14]**:** M^+ 400. Elemental analysis of Anal. Calcd. For $C_{24}H_{20}N_2O_4$% (400.14): C, 71.99; H, 5.03; N, 7.00. Found: C, 71.95; H, 5.03; N, 6.95.

2.1.2. **DMPCH-1**:

Anhydrous 1-pentanol (5 mL) was taken in 25 mL RB flask. To this was added **2** (1.0 g, 2.5 mmol), **3** (0.15 g, 0.84 mmol) and $Zn(OAc)_2$ (0.24 g, 1.092 mmol) was under nitrogen atmosphere. 1,8-diazabicyclo[5.4.0]undec-7-ene (DBU) (0.1 mL, 0.66 mmol) was added at 100^0 C and the resultant solution was heated to 140^0 C for 20 h and then cooled to room temperature. Pentanol was removed under high vacuum and the solid green material was precipitated from methanol which was then subjected to silica gel column chromatography and eluted with methanol-chloroform. The green phthalocyanine compound (second fraction) obtained was reprecipitated from methanol to afford the pure compound in 8% yield (0.097 g) for this isomer. FT-IR (KBr) υ_{max} 3413, 2928, 2840, 1713, 1254, 1024 cm^{-1}. UV-Vis: (in THF, λ_{max}, ε $M^{-1}cm^{-1}$): 691(91,100), 623(18,200), 354(34,800). ESI-MS (*m*/z): $C_{81}H_{64}N_8O_{14}Zn$ [1436.38]: $[M-H]^+$ 1435. Elemental analysis of Anal. Calcd. For $C_{81}H_{64}N_8O_{14}Zn$ % (1436.38): C, 67.62; H, 4.48; N, 7.79. Found: C, 67.71; H, 4.52; N, 7.94.

2.1.3. **DMPCH-2**:

Anhydrous 1-pentanol (5 mL) was taken in 25 mL RB flask. To this was added **2** (1.0 g, 2.5 mmol), **4** (0.310 g, 0.84 mmol) and $Zn(OAc)_2$ (0.240 g, 1.092 mmol) under nitrogen atmosphere. To this catalytic amount of DBU (0.1 mL, 0.66 mmol) was added at 100 ^{0}C and the resultant solution was heated to 140^0 C for 20 h and cooled to room temperature. Pentanol was removed under high vacuum. Solid material obtained was subjected to silica gel column chromatography and eluted with hexane-chloroform. The second fraction was collected and reprecipitated from methanol to get **5** in 9% yields (0.12 g) for this particular isomer. FT-IR (KBr) υ_{max} 2930, 2839, 1728 (CO stretching), 1249, 1026 cm^{-1}. ESI-MS (*m*/*z*): $C_{91}H_{80}N_8O_{18}Zn$ [1639]: (M^+) 1640. Elemental analysis of Anal. Calcd. For $C_{91}H_{80}N_8O_{18}Zn$ % (1639.05): C, 66.68; H, 4.92; N, 6.84. Found: C, 66.65; H, 4.95; N, 6.85.

The desired compound was obtained by the hydrolysis of **5** using Na/Ethanol. 100 mg of compound **5** was dissolved in 30 mL of ethanol. To this 1 g (43.3 mmol) of sodium was added. The resulting reaction mixture was stirred at room temperature for 7 days under nitrogen atmosphere. The solvent was removed under reduced pressure. The obtained solid material was dissolved in water and the pH was adjusted to 2-3 by adding dil. HCl. The precipitate was filtered and dried under vacuum to get the desired product in 92% yield (0.85 g). FT-IR (KBr) υ_{max} 1719 (CO stretching) cm^{-1}. UV-Vis: (in THF, λ_{max}, ε $M^{-1}cm^{-1}$): 691(1,35,100), 623 (24,500), 355 (47,600). ESI-MS (*m*/*z*): $C_{84}H_{68}N_8O_{16}Zn$ [1510]: (M^+) 1511.5, Elemental analysis of Anal. Calcd. For $C_{84}H_{68}N_8O_{16}Zn$ % (1510.87): C, 66.78; H, 4.54; N, 7.42. Found: C, 66.75; H, 4.50; N, 7.45.

2.1.4. 4,5-Bis(2,6-dimethoxyphenoxy) phthalonitrile **(6):**

Dry DMF (15 mL) was taken in 50 mL RB flask. To this was added 2,6-dimethoxyphenol (3.126 g, 20.30 mmol), 4,5-dichlorophthalonitrile (1.0 g, 5.076 mmol), K_2CO_3 (7.015 g, 50.76 mmol) and the resultant reaction mixture was heated at 100^{o}C under nitrogen atmosphere for 48 h. The reaction mixture was poured into water and the aqueous layer was extracted three times with dichloromethane and dried over anhydrous Na_2SO_4. The organic layer was evaporated and the residue was purified by silica gel column chromatography by eluting with Hexane-Ethyl acetate to get the pure compound as white solid in 85% yield (1.85 g). FT-IR (KBr) υ_{max} 2229 (CN) cm^{-1}. ^{1}H NMR ($CDCl_3$, 300MHz): δ (ppm) 7.9 (s, 2H), 6.9 (s, 2H), 6.82(d, J= 8.30 Hz, 4H), 3.78 (s, 12H). ESI-MS (*m*/*z*): $C_{24}H_{20}N_2O_6$ [432.13]: (M+1) 433.

2.1.5. **DMPCH-3**:

Anhydrous 1-pentanol (10 mL) was taken in 25 mL RB flask. To this was added 4,5-bis(2,6-dimethoxyphenoxy)phthalonitrile (0.900 g, 2.08 mmol), 4-(1,1,2-tricarbethoxyethyl) phthalonitrile (0.260 g ,0.695 mmol), $Zn(OAc)_2$ (0.240 mg ,0.9 mmol) and catalytic amount of DBU and the reaction mixture was heated under reflux for 20 h under nitrogen atmosphere. The solvent was then removed under reduced pressure and the green solid material obtained was subjected to column chromatography using silica gel (100-200 mesh) by eluting with $CHCl_3$-Hexane. The second green band was collected as the desired product (**7**) and recrystallized from methanol to obtain the pure compound in 8% yield (0.10 g) for this particular isomer. FT-IR (KBr) υ_{max} 1727 (-COOEt) cm^{-1}. ESI-MS (*m*/*z*): $C_{92}H_{83}N_8O_{24}Zn$ [1748.48]: M^+ 1748.

The desired unsymmetrical phthalocyanine was obtained by hydrolysis of **7** using Na/Ethanol. Ethanol (20 mL) was taken in a dry two neck RB flask and to this 1 gm (43.4 mmol) of sodium was added and allowed to dissolve. Then 100 mg of **7** was dissolved in THF-Ethanol solvent mixture. The resulting reaction mixture was stirred at room temperature for 7 days. The solvent was evaporated under reduced pressure. The obtained solid material was dissolved in water and pH was adjusted to 2-3 by using dil.HCl. The precipitate was filtered and dried under reduced pressure to get the desired product in 80% yield (0.086 g). FT-IR (KBr) υ_{max} 1713 (-COOH) cm^{-1}. ESI-MS (*m*/*z*): $C_{84}H_{68}N_8O_{22}Zn$ [1606.87]: $[M-2H]^+$ 1604, UV-Vis: (in **DCM**, λ_{max}, ε $M^{-1}cm^{-1}$): 686 (1,50,000), 649 sh (31,000), 614 (36,000), 360 (85,000). For $C_{84}H_{68}N_8O_{22}Zn$ % (1606.87): C, 62.79; H, 4.27; N, 6.97. Found: C, 62.84; H, 4.22; N, 6.99.

2.2. Methods

The UV-Visible spectra were recorded with Ocean Optics spectrophotometer using for 1 x 10^{-6} M solutions in THF solvent. Steady state fluorescence spectra were recorded using a Spex model Fluorlog-3 spectrofluorometer for solutions having optical density at the wavelength of excitation (λ_{ex}) ≈ 0.11. Time-resolved fluorescence measurements have been carried out using HORIBA Jobin Yvon spectrofluorometer. Briefly, the samples were excited at 370 nm and the emission was monitored at 700 nm, in all unsymmetrical phthalocyanines. The count rates employed were typically $10^3 – 10^4$ s^{-1}. Deconvolution of the data was carried out by the method of iterative reconvolution of the instrument response

function and the assumed decay function using DAS-6 software. The goodness of the fit of the experimental data to the assumed decay function was judged by the standard statistical tests (*i.e.*, random distribution of weighted residuals, the autocorrelation function and the values of reduced χ^2). ^{1}H NMR spectra were obtained at 300 MHz using a Brucker 300 Avance NMR spectrometer running X-WIN NMR software. The elemental analyses were done on an Elementar, Vario MICRO CUBE analyzer.

Differential pulse and cyclic voltammetric measurements were performed on a PC-controlled CH instruments model CHI 620C electrochemical analyzer. Cyclic voltammetric experiments were performed on 1 mM unsymmetrical phthalocyanine solution in THF solvent at scan rate of 100 mV/s using 0.1 M tetrabutyl ammonium perchlorate (TBAP) as supporting electrolyte. The working electrode is glassy carbon, standard calomel electrode (SCE) is reference electrode and platinum wire is an auxiliary electrode. After a cyclic voltammogram (CV) had been recorded, ferrocene was added, and a second voltammogram was measured. Spectroelectrochemical experiments were performed using a CH instruments model CHI 620C electrochemical analyzer utilizing a three-electrode configuration of thin layer quartz spectroelectrochemical cell at 25 °C. The working electrode was transparent Pt gauze. Pt wire counter electrode and SCE reference electrode separated from the bulk of the solution by a double bridge were used. The TG curves of the samples were performed on a thermogravimetric analyzer Mettler Tolledo TGA/SDTA 851^c under nitrogen atmosphere (99.999%) from 25 to 600 ^{o}C, in Al_2O_3 crucibles. The heating rates were 10 ^{o}C/min and the flow rate of nitrogen was 80 mL/min.

2.2.1. Dye cell preparation

The detailed TiO_2 photoelectrode (area: ca. 0.740 cm^2) preparation was described in our earlier studies [20,21]. Briefly, nanocrystalline TiO_2 films of 8 – 10 μm thickness with porosity of 68% were deposited onto transparent conducting glass (Nippon Sheet Glass, which has been coated with a fluorine-doped stannic oxide layer, sheet resistance of 8-10 Ω/cm^2) over which ~4.5 μm thickness of 400 nm anatase TiO_2 particles (CCIC, HPW-400) as scattering layer by screen-printing. These films were gradually sintered at 500 ^{o}C for 30 min. The heated electrodes were impregnated with a 0.04 M titanium tetrachloride solution in water saturated desiccator for 30 min at 70 ^{o}C and then washed with distilled water and rinsed with ethanol. The electrodes were heated again at 500 ^{o}C for 30 min and then allowed to cool

to 50 ^{o}C before dipping them into the dye solution (3 x 10^{-6} M in THF). The electrodes were dipped into the dye solution for >18 h at 25 ^{o}C. The dye sensitized TiO_2 electrodes were assembled with Pt counter electrodes by heating with a hot-melt surlyn film (Surlyn 1702, 25 μm thickness, Du-Pont) as a spacer in-between the electrodes. A liquid electrolyte, consisted of 0.6 M 1,3-dimethylimidazolium iodide, 0.03 M iodine, 0.05 M LiI, 0.05 M guanidinium thiocyanate, and 0.25 M 4-*tert*-butylpyridine in 15/85 (v/v) mixture of valeronitrile and acetonitrile was filled through the predrilled hole present on the counter electrode and then the hole was sealed with a Surlyn disk and a thin glass to avoid leakage of the electrolyte.

The photovoltaic performance of these devices were characterized under irradiation source of 450 W xenon light source (Osram XBO 450, U.S.A.), which is equivalent to an AM 1.5 solar simulator and was calibrated by using a Tempax 113 solar filter (Schott). In order to reduce scattered light from the edge of the glass electrodes of the dyed TiO_2 layer, a light shading black mask was used onto the DSSCs. For photovoltaic measurements of the DSSCs, the irradiation source was a 450 W xenon light source (Osram XBO 450, Germany) with a filter (Schott 113), whose power was regulated to the AM 1.5G solar standard by using a reference Si photodiode equipped with a color matched filter (KG-3, Schott) in order to reduce the mismatch in the region of 350-750 nm between the simulated light and AM 1.5G to less than 4%. The measurement of incident photon-to-current conversion efficiency (IPCE) was plotted as a function of excitation wavelength by using the incident light from a 300 W xenon lamp (ILC Technology, USA), which was focused through a Gemini-180 double monochromator (Jobin Yvon Ltd.). The measurement settling time between applying a voltage and measuring a current for the I-V characterization of DSSCs was fixed to 40 ms.

2.3. Computational methodology

DFT and TD-DFT calculations have been carried in solution (THF) using the Gaussian09 code [22]. The Becke's hybrid exchange functional B3 [23] with the Lee–Yang–Parr correlation functional LYP [24,25] (B3LYP) have been used in our calculations together with the 6-31G** basis set. [26] The solvation effects have been included by means of the conductor-like polarizable continuum model CPCM [27-29]. The lowest 100 singlet-singlet excitations have been computed on the fully optimized geometries and transition energies and oscillator strengths convoluted with a Gaussian function of sigma=0.20.

3. Results and Discussions

The syntheses of the new sterically demanded unsymmetrical phthalocyanines are shown in schemes 1 & 2. The phthalonitrile, 4,5-bis(3,4-dimethoxy) phthalonitrile (**2**) was synthesized by using a Suzuki coupling reaction [30]. In contrast, the phthalonitrile, 4,5-bis(2,6-dimethoxyphenoxy) phthalonitrile (**6**) was synthesized by an aromatic nucleophilic substitution reaction between 2,6-dimethoxy phenol and 4,5-dichlorophthalonitrile. All three sterically demanded unsymmetrical phthalocyanines were synthesized by cross-condensation of two different phthalonitriles. For example, **DMPCH-1** was synthesized by cross-condensation of **2** and **3** using $Zn(OAc)_2$ as metal template. On the other hand **DMPCH-2** & **3** was obtained by cross-condensation of **4** with either **2** or **6** phthalonitriles, respectively. In all three unsymmetrical phthalocyanines, six different isomers were formed but, we have isolated only the required isomer (*i.e.*, A3B) and remaining isomers were discarded [31]. The new unsymmetrical phthalocyanines were characterized by elemental analysis, Mass, IR, ^{1}H NMR, and fluorescence spectroscopies (both steady-state and time-resolved) as well as cyclic voltammetry (including spectroelectrochemistry).

The mass spectrum of each of unsymmetrical phthalocyanine shows the molecular ion peak, which correspond to the presence of respective unsymmetrical phthalocyanine. Figure 2 shows the absorption spectra of all three unsymmetrical phthalocyanines using THF solvent and the corresponding data are presented in Table 1. The UV-Visible absorption spectroscopy is a very valuable technique which can be used to study the aggregation phenomena of phthalocyanines in both solution and solid state. As frequently encountered in most phthalocyanines, the shoulder on the high energy side of the Q-band indicates the presence of aggregated species [32,33]. As shown in Figure 2, all three unsymmetrical phthalocyanines have shown a very intense Q-band whereas the band at higher energy side of the Q-band is very low intensity. This clearly indicates that the aggregation of these unsymmetrical phthalcoyanines in THF solution is low. Moreover, the theoretical absorption spectra computed on the monomers are in very good agreement with the experimental ones further confirming the low presence of aggregates in THF solution. Absorption spectra of **DMPCH-3** shows split in the Q-band region. This is probably due to the presence of more bulky groups in **DMPCH-3** than other unsymmetrical phthalocyanines. A similar split in Q-bands was also observed in other sterically hindered unsymmetrical phthalocyanines [16]. Figure 3 represents the emission spectra of all three unsymmetrical phthalocyanines obtained at room temperature in THF solvent. The emission maxima were presented in Table 1. The

excitation spectrum obtained by exciting emission maximum at 765 nm shows a maximum at 697 nm and $E_{0\text{-}0}$ energy of these unsymmetrical phthalocyanines estimated from excitation and emission spectra are 1.78, 1.79 & 1.80 eV for **DMPCH-1**, **DMPCH-2** & **DMPCH-3**, respectively. Quenched emission spectra were observed in all three unsymmetrical phthalocyanines when adsorbed onto 2 μm thick TiO_2 layer as a consequence of electron injection from the excited state of phthalocyanine into conduction band of TiO_2. The singlet excited life-time of all three unsymmetrical phthalocyanines were measured in THF solvent and were found to be 2.70, 3.11 & 2.86 ns for **DMPCH-1**, **DMPCH-2** & **DMPCH-3**, respectively. In all three cases the excited state life-time quenched when adsorbed onto 2 μm thick TiO_2 layer.

With a view to evaluate the HOMO-LUMO levels of unsymmetrical phthalocyanines, we performed the electrochemistry by using cyclic and differential pulse voltammetric techniques in THF solvent. Each of unsymmetrical phthalocyanine undergoes either reversible or quasireversible oxidation at 0.60, 0.65 and 0.80 Vs. SCE generating π-cation radical for **DMPCH-1**, **DMPCH-2** & **DMPCH-3**, respectively. The cyclic voltammogram (CV, solid line) and differential pulse voltammogram (DPV, dotted line) of **DMPCH-1** are shown in Figure 4. In a similar manner each unsymmetrical phthalocyanine undergoes either two or three reversible or quasireversible reductions (complete data in Table 1). With respect to dye-sensitization of wide-band-gap semiconductors, e.g. TiO_2, the oxidation potentials of unsymmetrical phthalocyanines and the $E_{0\text{-}0}$ transition energy, the energy levels of the singlet excited states (excited state oxidation potential) of **DMPCH-1, DMPCH-2** & **DMPCH-3** were determined to be -1.18, -1.14 & -1.00 V vs. SCE, respectively [34]. Whereas the energy level of the conduction band edge of TiO_2 is ca. –0.74 V vs. SCE [35]. This makes electron injection from the excited state of unsymmetrical phthalocyanines into the conduction band of TiO_2 thermodynamically feasible. Furthermore, the HOMO level of the unsymmetrical phthalocyanines is lower than the energy level of the redox couple I^-/I_3^- (0.2 V vs. SCE) in the electrolyte, enabling the dye regeneration by electron transfer from iodide ions in the electrolyte.

3.1. Spectroelectrochemical Studies

Spectroelectrochemical studies were employed to monitor changes during redox reactions as well as assignments in the CVs of unsymmetrical phthalocyanines. This

information is essential concerning the durability of the sensitizer. Figure 5 shows the spectral changes of **DMPCH-2** under applied potential. During the controlled potential oxidation of DMPCH-**2** at 0.90 V applied potential, the absorption of both Q-band and Soret band decreases in intensity without shift, while new bands appeared at 510 and 744 nm with increase in intensity. The band assigned to the aggregated species at 623 nm is also decreases in intensity due to the shifting of the aggregation-disaggregation equilibrium under applied potential. During this electrochemical oxidation, clear isosbestic points are observed at 343, 413, 612, 639 and 713 nm, which demonstrates that oxidation gives a single product. These spectroscopic changes indicate presence of aggregation-disaggregation equilibrium and a macrocycle ring oxidation process and the oxidation process assigned to $[Zn^{II}Pc^{-2}]/[Zn^{II}Pc^{-1}]^{+1}$ process [36-38]. The unsymmetrical phthalocyanine return to their original absorption spectrum, when the applied potential is removed. During the reduction of **DMPCH-2** (applied potential at -1.2 V), the absorption of the both the Q-band and Soret band intensities increases without shift. In contrast, the intensity of the peak at 623 nm decreases, which indicates disaggregation of the phthalocyanine macrocycle. During this process clear isosbestic points are observed at 348, 401, 616 and 707 nm, which clearly indicates that the reduction gives a single product. These changes are typical of the ring-based reduction and assigned to $[Zn^{II}Pc^{-2}]/[Zn^{II}Pc^{-3}]^{-1}$. Spectroscopic changes under controlled potential application at -1.80 V supported the further reduction of the monoanionic $[Zn^{II}Pc^{-3}]^{-1}$ species to $[Zn^{II}Pc^{-4}]^{-2}$. Similar spectroscopic changes are observed in the case of **DMPCH-1** also during the controlled applied potential (*see* Supplementary data).

Figure 6 indicates *in-situ* spectral changes of **DMPCH-3** in THF solvent during the applied potential. When the applied potential is at 0.90 V, the Q-band at 683 nm decreases in intensity with a blue-shift to 679 nm. On the other hand the Soret band at 363 nm increases the intensity with a blue-shift to 353 nm and appearance of a new band at 466 nm. This process gives clear isosbestic points at 399, 624, & 676 nm in the spectra, which indicates the oxidation process give a single product. Figure 6b represents the spectral changes during the reduction process of the phthalocyanine macrocycle. During -1.0 V potential application, the intensity of both the Q-band and the Soret band decreases with the change in absorption maxima. The reduction process assigned to $[Zn^{II}Pc^{-2}]/[Zn^{II}Pc^{-1}]^{+1}$ with isosbestic points at

332, 419, 607 & 701 nm. Further reduction of $[Zn^{II}Pc^{-3}]^{-1}$ at -1.70 V indicates further decreases in intensity of the Q-band, whereas the Soret band becomes a shoulder with the appearance of new band at 550 nm. This process gives the isosbestic points at 303, 398, 607, 632 & 711 nm. Both first and second reduction belongs to the macrocycle reductions.

3.2. Computational Studies

To gain insight into the electronic and optical properties of the investigated compounds, we performed DFT/TDDFT calculations in THF on the optimized geometries. The results are reported in terms of schematic energy diagram and isodensity plots of frontier molecular orbitals in Figure 7 and 8. The computed TDDFT absorption spectra absorption in THF are compared to the experimental ones in Figure 9 while a survey of the most relevant excited states are compiled in Table 2, 3 and 4.

From Figure 7 we notice the trends of HOMO energies reproduce the decreased (*i.e.* less positive) oxidation potential measured for **DMPCH-3** compared to **DMPCH-1** and **DMPCH-**2 which have almost the same oxidation potential. Also in line with electrochemical measurements a higher lying LUMO is calculated for **DMPCH-3** compared to **DMPCH-1** and **DMPCH-2**, probably as a result of the increased donation to the macrocyle. For all the investigated systems the HOMO (H) is delocalized on the π-electron system of the phthalocyanine ring while the LUMO (L) is a π* orbitals delocalized on the phthalocyanine center and on the carboxyl group, Figure 8.

This electronic structure picture results in a lowest transition, S_1 (H→L), with a directional charge flow from the dye core to the anchoring group that facilitates the electron injection from the excited state of phthalocyanine macrocyle sensitizer to the conduction band of TiO_2. These results are in good agreement other phthalocyanine sensitizers reported in the literature [39]. For all the species the low energy has also a contribution from the second transition S_2 that has a H→L+1 character and similar oscillator strength than that of S_1. In this transition the arriving state L+1 that is also a π* orbital delocalized on the phthalocyanine center but contrarily to the L case it has no contribution from the anchoring group. On the other hand, for the **DMPCH-3**, possessing two different carboxylic groups, the charge delocalization of the LUMO extends only to one of the two groups and this could lead to a loss in the charge generation with respect to that of **DMPCH-1** and **DMPCH-2**

depending on which is the preferred anchoring site. On overall, the computed spectra are in good agreement with the experimental band though blue-shifted with respect to the experiment, especially for the **DMPCH-3** species. Calculations on the isolated molecule models do not show the presence of the shoulder at ca. 630 nm confirming its assignment to the phthalocyanines aggregates, based on the spectroelectrochemistry measurements, see above.

3.3. Photoelectrochemical Studies

Due to the favorable photophysical properties, electrochemical properties and the energy profile with respect to the conduction band edge of TiO_2 and the redox system, which are further supported by our TD-DFT studies, the photovoltaic performance of unsymmetrical phthalocyanines were evaluated by constructing DSSC using nanocrystalline TiO_2 films and I^-/I^{3-} redox electrolyte system and the results are shown in Table 5. The overall conversion efficiency (η) is calculated from the J_{SC}, V_{OC}, FF and intensity of incident light (I_{ph}), using the equation below.

$$\eta[\%] = \frac{J_{SC}[mAcm^{-2}].V_{OC}[V]Xff}{I_{ph}} \text{x}100$$

As tabulated in Table 5, the short-circuit current density (J_{SC}), open-circuit voltage (V_{OC}), and fill factor (ff) of **DMPCH-2** based DSSC under an irradiance of AM 1.5G are 3.26 mA/cm2, 0.604 V and 0.67, respectively, yielding an overall conversion efficiency of 1.07%. Similarly, we have observed an overall conversion efficiency of 0.89, & 0.74% using **DMPCH-1**, & **DMPCH-3** based sensitizers, respectively.

3.4. Thermogravimetric studies

Finally, we have examined the thermal stability of the new unsymmetrical phthalocyanines by using thermogravimetric analysis for outdoor applications. Figure 10 shows the thermal behavior of **DMPCH-1**. It is known from the literature that phthalocyanine and its metallo derivatives are stable up to 400 ^oC [40]. The thermograme indicates that the **DMPCH-1** sensitizer is stable up to 250 ^oC. The initial weight loss (3.00 %) was observed in 150 - 300 ^oC temperature and is attributed to the removal of moisture and after that weight loss was due to the removal of the carboxyl group from the macrocycle. Similar

thermogrames are obtained with **DMPCH-2** & **DMPCH-3** sensitizers (*See* supporting information & Table 6).

4. Conclusions

In conclusion, we have designed three sterically demanding unsymmetrical phthalocyanines for dye-sensitized solar cells. The absorption maxima of these phthalocyanines are located at 690 nm in THF solvent and the emission maxima at around 700 nm with excited state life-time of 2.70, 3.11 & 2.86 ns for **DMPCH-1**, **DMPCH-2** & **DMPCH-3**, respectively. Both emission intensity and excited state life-time was quenched when adsorbed onto TiO_2 films, a feature indicates that there is an efficient electron transfer from excited state of macrocycle to TiO_2 conduction band. Spectroelectrochemical studies indicate that the electron transfer processes are ring-centered and not metal-centered processes. All three unsymmetrical phthalocyanines were tested in DSSC using I^-/I_3^- redox couple and offered low overall conversion efficiencies of ca. 1.1%.

Acknowledgements

The authors are thankful to the joint DST-EU project 'ESCORT' (FP7-ENERGY-2010, contract no. 262910) for the financial support of this work. The author VKS thanks to CSIR for senior research fellowship.

References:

[1] Branker K, Pathak JKM, Pearce JM, A Review of solar photovoltaic levelized cost electricity. Renewable and Sustainable Reviews 2011; 15: 4470-82.

[2] O'Regan B, Grätzel M, A low-cost, high efficiency solar cell based on dye-sensitized colloidal TiO_2 films. Nature 1991; 353: 737-40.

[3] Grätzel M, Recent advances in sensitized mesoscopic solar cells. Acc. Chem. Res. 2009; 42: 1788-98.

[4] Giribabu L, Kanaparthi RK, Velkannan V, Molecular engineering of sensitizers for dye-sensitized solar cell applications. The Chem. Record 2012; 12: 306-28.

[5] Nazeeruddin MK, Pechy P, Renouard T, Zakeeruddin SM, Humphry-Baker R, Comte P, Liska P, Cevery L, Costa E, Shklover V, Spiccia L, Deacon GB, Bignozzi CA, Grätzel M, Engineering of efficient panchromatic sensitizers for nanocrystalline TiO_2 based solar cells. J. Am. Chem. Soc., 2001; 123: 1613-24.

[6] Han L, Islam A, Chen H, Chandrasekharam M, Chiranjeevi B, Zhang S, Yang X, Yanagida M, High-efficiency dye-sensitized solar cell with a novel co-adsorbent. Energy Environ. Sci. 2012; 5: 6057-60.

[7] Campbell WM, Burrell AK, Officer DL, Jolley KW, Porphyrins as light harvesters in dye-sensitized TiO_2 solar cell. Coord. Chem. Rev.2004; 248: 1363-79.

[8] Himahori H, Umeyama T, Ito S, Large π-aromatic molecules as potential sensitizers for highly efficient dye-sensitized solar cells. Acc. Chem. Res. 2009; 42: 1809–18.

[9] Giribabu L, Sudhakar K, Velkannan V, Phthalocyanines: potential alternative sensitizers to Ru(II) polypyridyl complexes for dye-sensitized solar cells. Current Sci. 2012; 102: 991-00.

[10] Yella A, Lee HW, Tsao HN, Yi C, Chandiran AK, Nazeeruddin MK, Diau EWG, Yeh CY, Zakeeruddin SM, Grätzel M, Porphyrin-sensitized solar cells with Cobalt(II/III)-based redox electrolyte exceed 12 percent efficiency. Science 2011; 334: 629-34.

[11] deLaTorre G, Claessens CG, Torres T, Phthalocyanines: old dyes, new materials. Putting color in nanotechnology Chem. Commun. 2007; 2000-15.

[12] Mack J, Kobayashi N, Low symmetry phthalocyanines and their analogues. Chem.Rev. 2011; 111: 281-321.

[13] Reddy PY, Giribabu L, Lyness C, Snaith H, Vijaykumar C, Chandrasekharam M, Lakshmikantam M, Yum JH, Kalyanasundaram K, Grätzel M, Nazeeruddin MK, Efficient sensitization of nanocrystalline TiO2 films by a near-IR absorbing unsymmetrical zinc phthalocyanine. Angew. Chem. Int. Ed. 2007; 46: 373-6.

[14] Giribabu L, Vijaykumar Ch, Reddy VG, Reddy PY, Rao Ch S, Jang SR, Yum JH, Nazeeruddin MK, Grätzel M, Unsymmetrical alkoxy zinc phthalocyanine for

sensitization of nanocrystalline TiO_2 films. Solar Energy Materials & Solar Cells. 2007; **91**: 1611-7.

[15] Mori S, Nagata M, Nakahata Y, Yasuta K, Goto R, Kimura M, Taya M, Enhancement of incident photon-to-current conversion efficiency for phthalocyanine-sensitized solar cells by 3D molecular structuralization. J. Am. Chem. Soc. 2010; 132: 4054-5.

[16] Ragoussi ME, Cid JJ, Yum JH, delaTorre G, Censo DD, Grätzel M, Nazeeruddin MK, Torres T, Carboxyethynyl anchoring ligands: a means to improving the efficiency of phthalocyanine-sensitized solar cells. Angew. Chem. Int. Ed. 2012; 51: 1-5.

[17] "Purification of Laboratory Chemicals," Ed.'s W.L.F. Armango, Ch.L.L. Chai 2003, Butterworth Heinemann, NewYork.

[18] Kasim M, Gul A, Kocak M, Synthesis of tetra(tricarboxy)- and tetra(dicarboxy)-substituted soluble phthalocyanines. J. Porphyrins Phthalocyanines, 2003; 7: 617-22.

[19] Minshi A, Soonwha K, Jong-Dal H. Bull. Korean Chem. Soc. 2010; 31: 3272-78.

[20] Giribabu L, Bessho T, Srinivasu M, Vijaykumar C, Soujanya Y, Reddy VG, Reddy PY, Yum JH, Grätzel M, Nazeeruddin MK, A new family of heteroleptic ruthenium(II) polypyridyl complexes for sensitization of nanocrystalline TiO_2 films. Dalton Trans. 2011; 40: 4497-504.

[21] Giribabu L, Vijaykumar Ch, Reddy PY, Yum JH, Grätzel M, Nazeeruddin MK, Unsymmetrical extended π-conjugated zinc phthalocyanine for sensitization of nanocrystalline TiO_2 films. J. Chem. Sci., 2009: 121: 75–82.

[22] Gaussian 09, Revision **A.1**, Frisch MJ, Trucks GW, Schlegel HB, Scuseria GE, Robb MA Cheeseman JR, Scalmani G, Barone V, Mennucci B, Petersson GA, Nakatsuji H, Caricato M, Li X, Hratchian HP, Izmaylov AF, Bloino J, Zheng G, Sonnenberg JL, Hada M, Ehara M, Toyota K, Fukuda R, Hasegawa J, Ishida M, Nakajima T, Honda Y, Kitao O, Nakai H, Vreven T, Montgomery Jr., JA, Peralta J.E, Ogliaro F, Bearpark M, Heyd JJ, Brothers E, Kudin KN, Staroverov VN, Kobayashi R, Normand J, Raghavachari K, Rendell A, Burant JC, Iyengar SS, Tomasi J, Cossi M, Rega N, Millam JM, Klene M, Knox JE, Cross JB, Bakken V, Adamo C, Jaramillo J,

Gomperts R, Stratmann RE, Yazyev O, Austin AJ, Cammi R, Pomelli C, Ochterski JW, Martin RL Morokuma K, Zakrzewski VG, Voth GA, Salvador P, Dannenberg JJ, Dapprich S, Daniels AD, Farkas Ö, Foresman JB, Ortiz JV, Cioslowski J, Fox DJ, Gaussian, Inc., Wallingford CT, 2009.

[23] Becke AD, Density functional thermochemistry III. The role of exact exchange. J. Chem. Phys. 1993; 98: 5648–52.

[24] Lee C, Yang W, Parr RG, Development of the Colle-Salvetti correlation-energy formula into a functional of the electron density. Phys. Rev. B. 1998; 37: 785–9.

[25] Miehlich B, Savin A, Stoll H, Preuss H, Results obtained with the correlation energy density functionals of becke and Lee, Yang and Parr. Chem. Phys. Lett. 1989; 157: 200–6.

[26] Petersson GA, Al-Laham MA, A complete basis set model chemistry II. Open-shell systems and the total energies of the first-row atoms. J. Chem. Phys. 1991; 94: 6081-90.

[27] Cossi M, Rega N, Scalmani G, Barone V, Energies, structures, and electronic properties of molecules in solution with the C-PCM solvation model . J. Comput. Chem. 2003, 24, 669–81.

[28] Cossi M, Barone V, Separation between fast and slow polarizations in continuum solvation models. J. Phys. Chem. A 2000; 104: 10614–22.

[29] Cossi M, Barone V, Time dependent density functional theory for molecules in liquid solutions. J. Chem. Phys. 2001; 115: 4708–17.

[30] Suzuki A, Recent advances in the cross-coupling reactions of organoboron derivatives with organic electrophiles, 1995–1998. J. Organo. Metallic Chem. 1999; 576: 147-68.

[31] Akkurt HYY, Okur AI, Gul A, Unsymmetrical phthalocyanines with cyclopalladated azo functions. J. Porphyrins & Phthalocyanines 2012; 16: 192-199.

[32] Goslinski T, Osmalek T, Konopka K, Wierzchowski M, Fita P, Mielcarek J, Photophysical properties and photocytotoxicity of novel phthalocyanines – potentially useful for their application in photodynamic therapy. Polyhedron 2011; 30: 1538-1546.

[33] Manna H, Tuhl A, Samuel J, Al-Mulla A, Al-Awadi NA, Makhseed S, Photophysical and nonlinear optical properties of zincphthalocyanines with peripheral substitutions. Optics Commun. 2011; 248: 450-454.

[34] Excited state oxidation potentials are calculated by using $E^* = E_{1/2(OX)}-E_{0-0}$.

[35] Hagfeldt A, Grätzel M, Light induced redox reactions in nanocrystalline systems. Chem. Rev. 1995; 95: 49-68.

[36] Simicglavaski B, Zecevic S, Yeager E. Spectroelectrochemical in-situ studies of phthalocyanines. J Electrochem Soc 1987;134: C130.

[37] Agboola B, Ozoemena KI, Nyokong T. Synthesis and electrochemical characterization of benzylmercapto and dodecylmercapto tetra substituted cobalt, iron, and zinc phthalocyanines complexes. Electrochim Acta 2006; 51: 4379-87.

[38] Ou Z, Jiang Z, Chen N, Huang J, Shen J, Kadish KM, Synthesis, electrochemistry and spectroelectrochemistry of tetra-α-substituted metallophthalocyanines. J. Porphyrins & Phthalocyanines 2008; 12: 1123-33.

[39] Zanotti G, Angilini N, Paoletti AM, Pennesi G, Rossi G, Bonapasta AA, Mattioli G, Carlo AD, Brown TM, Lembo A, Reale A, Synthesis of novel unsymmetrical Zn(II) phthalocyanine bearing a phenyl ethynyl moiety as sensitizer for dye-sensitized solar cells. Dalton Trans. 2011; 40: 38-40.

[40] Wei X, Du X, Chen D, Chen Z, Thermal analysis study of 5,10,15,20-tetrakis (methoxyphenyl) and their nickel complexes, Thermochimica Acta, 2006; 440: 181-7 (and references therein).

Table 1. UV-Visible, Emission and Electrochemical Data[a]

Compound	Absorption[b]	Emission	$E_{0\text{-}0}$(eV)[c]	Potential V vs. SCE[d]	
	λ_{max}, nm (log ε M^{-1} cm^{-1})	λ_{max}, nm		Oxidation	Reduction
DMPCH-1	691(4.96), 623 (4.26), 354 (4.54).	701, 774	1.78	0.60	-1.02, -1.60, -1.87
DMPCH-2	691(5.13), 623 (4.39), 355 (4.68).	699, 772	1.79	0.65	-1.22, -1.67
DMPCH-3	686 (5.18), 649(sh) 614 (4.56), 360 (4.93).	688, 773	1.80	0.80[e]	-0.96, -1.41[e]

[a] Solvent THF. [b] Error limits: λ_{max}, ± 1 nm, log ε, ± 10%. [c] Error limits: ±0.05 eV. [d]Error limits, $E_{1/2}$, ± 0.03 V, 0.1 M TBAP.

Table 2. DMPCH-1 experimental and theoretical absorption maxima (nm/eV), computed transitions (nm/eV), oscillator strengths and composition in terms of molecular orbitals.

Exp.	Calc.	Trans	F	MO
680/1.83	662/1.88	671/1.85 (S_1)	0.6971	93% H→ L
		654/1.90 (S_2)	0.8291	92% H→ L+1
620/2.00 (sh)				
360/3.45	336/3.69	339/3.66 (S_{42})	0.7472	57% H→ L+5 21% H-14→ L
		337/3.68 (S_{43})	0.5724	32% H-14→ L 25% H→ L+5
		332/3.74 (S_{47})	0.4065	69% H→ L+6

Table 3. DMPCH-2 experimental and theoretical absorption maxima (nm/eV), computed transitions (nm/eV), oscillator strengths and composition in terms of molecular orbitals.

Exp.	Calc.	Trans	F	**MO**
680/1.83	668/1.86	682/1.82 (S1)	0.7442	95% H→ L
		656/1.89 (S2)	0.8313	93% H→ L+1
625/2.00 (sh)				
360/3.45	336/3.69	341/3.64 (S45)	0.2715	47% H→ L+6 10% H-17→ L
		341/3.64 (S46)	0.4370	24% H-17→ L+1 21% H-15→ L 10% H-18→ L 10% H→ L+5
		339/3.66 (S47)	0.2931	28% H→ L+5 23% H-15→ L 12% H-16→ L
		337/368 (S48)	0.3080	56% H-18→ L
		334/3.72 (S50)	0.5288	60% H→ L+6

Table 4. DMPCH-3 experimental and theoretical absorption maxima (nm/eV), computed transitions (nm/eV), oscillator strengths and composition in terms of molecular orbitals.

Exp.	Calc.	Trans	F	MO
720/1.72	665/1.86	665/1.86	0.7171	97% H→ L
689/1.80	620/2.00	620/2.00	0.5801	94% H→ L+1
623/1.99 (sh)				
400-500/3.10-2.48	456/2.72 (sh)	472/2.63	0.2709	52% H-3→ L 19% H-2→ L 17% H-1→ L
		444/2.79	0.2490	90% H-3→ L+1
375/3.31	336/3.69	361/3.43 (S_{38})	0.2730	76% H-19→ L
		348/3.56 (S_{44})	0.2818	56% H-19→ L+1 21% H-22→ L+1
		339/3.65 (S_{48})	0.3371	45% H-21→ L 26% H-20→ L 12% H-3→ L+2
		327/3.79 (S_{52})	0.5716	48% H-20→ L+1 11% H→ L+4 10% H→ L+5

Table 5: Photovoltaic performance data.[a]

Dye	Light Intensity	J_{SC} [mA cm^{-2}]	V_{OC} [V][a]	Fill factor (*ff*)[a]	η [%]
DMPCH-1	0.1	0.17	0.449	0.75	0.61
DMPCH-1	0.5	1.00	0.500	0.75	0.71
DMPCH-1	1	1.94	0.518	0.74	0.74
DMPCH-2	0.1	0.30	0.383	0.38	0.46
DMPCH-2	0.5	1.66	0.463	0.64	0.97
DMPCH-2	1	3.26	0.604	0.67	1.07
DMPCH-3	0.1	0.22	0.441	0.74	0.78
DMPCH-3	0.5	1.20	0.488	0.75	0.87
DMPCH-3	1	2.33	0.504	0.75	0.89

[a]Photoelectrode: TiO_2 (8 + 4 μm and 0.158 cm^2); Error limits: Short-circuit photocurrent density, J_{SC}, ±0.1 mAcm^{-2}, Open-circuit voltage, V_{OC}, ±30 mV, Fill factor, *ff* ±0.03; Electrolyte: 0.6 M 1,3-dimethylimidazolium iodide, 0.03 M iodine, 0.05 M LiI, 0.05 M guanidinium thiocyanate, and 0.25 M 4-*tert*-butylpyridine in 15/85 (v/v) mixture of valeronitrile and acetonitrile.

Table 6: Thermal decomposition data

Compound	Temperature rang (^{o}C)	Mass loss calculated (%)	Mass loss found (%)	Tentative assignment
DMPCH-1	25-300	3	1.25	Removal moisture
	300-600	23.33	4.39	Pc ring
DMPCH-2	25-220	3.45	1.19	Removal moisture
	220-600	44.75	6.89	Pc ring
DMPCH-3	25-220	13.05	1.12	Pc ring
	220-600	81.04	6.43	Pc ring

Figure Captions:

Fig. 1: Molecular structures of unsymmetrical phthalocyanines.

Fig. 2: UV-Visible spectra of (——) **DMPCH-1**, (------) **DMPCH-2** & (·····) **DMPCH-3** in THF solvent.

Fig. 3: Emission spectra (——) **DMPCH-1**, (------) **DMPCH-2** & (·····) **DMPCH-3** in THF solvent excitation at 690 nm.

Fig. 4: Cyclic (——) and differential (------) pulse voltammograms of **DMPCH-2**.

Fig. 5: *In-Situ* UV-Vis spectral changes of **DMPCH-2** a) E_{app} = 0.9 V. b) initial part of the spectral changes at E_{app} = -1.0 V, c) final part of the spectral changes at E_{app} = -1.70 V.

Fig. 6: *In-Situ* UV-Vis spectral changes of **DMPCH-3** a) E_{app} = 1.40 V. b) initial part of the spectral changes at E_{app} = -1.0 V, c) final part of the spectral changes at E_{app} = -1.70 V.

Fig. 7: Schematic representation of the energy levels for **DMPCH-1**, **DMPCH-2** and **DMPCH-3** in THF solution.

Fig. 8: Electronic distribution computed in THF for the first occupied/unoccupied molecular orbitals of the studied species.

Fig. 9: Computed vs. experimental absorption spectra in THF for **DMPCH-1** (top), **DMPCH-2** (center), **DMPCH-3** (bottom).

Fig. 10: TG/DTG curves of **DMPCH-1** with heating rate of 10 ^{o}C min-1 under nitrogen.

Scheme 1: Synthetic schemes of **DMPCH-1** & **DMPCH-2**.

Scheme 2: Synthetic scheme of **DMPCH-3**.

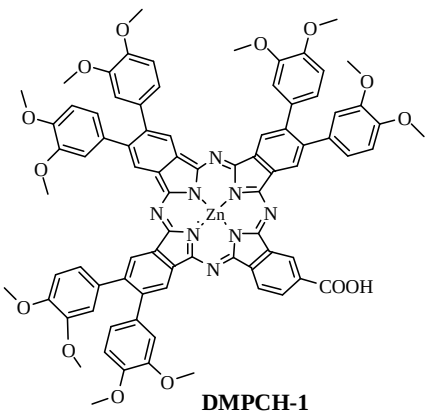

DMPCH-1

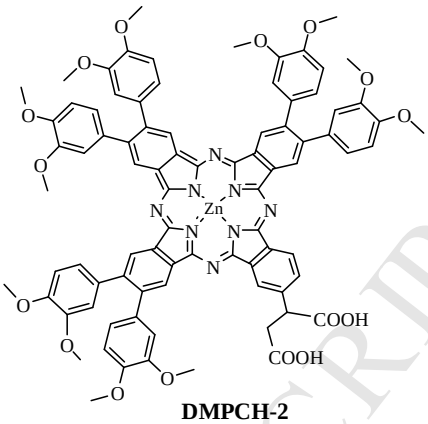

DMPCH-2

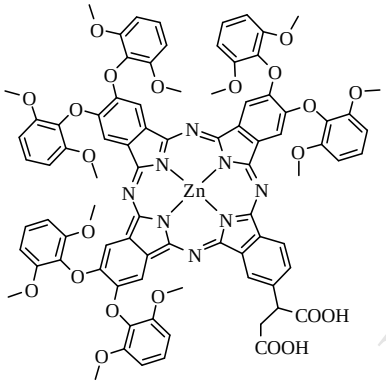

DMPCH-3

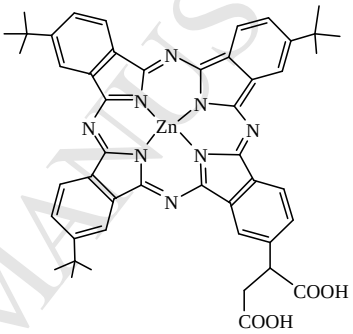

PCH-001

Figure 1

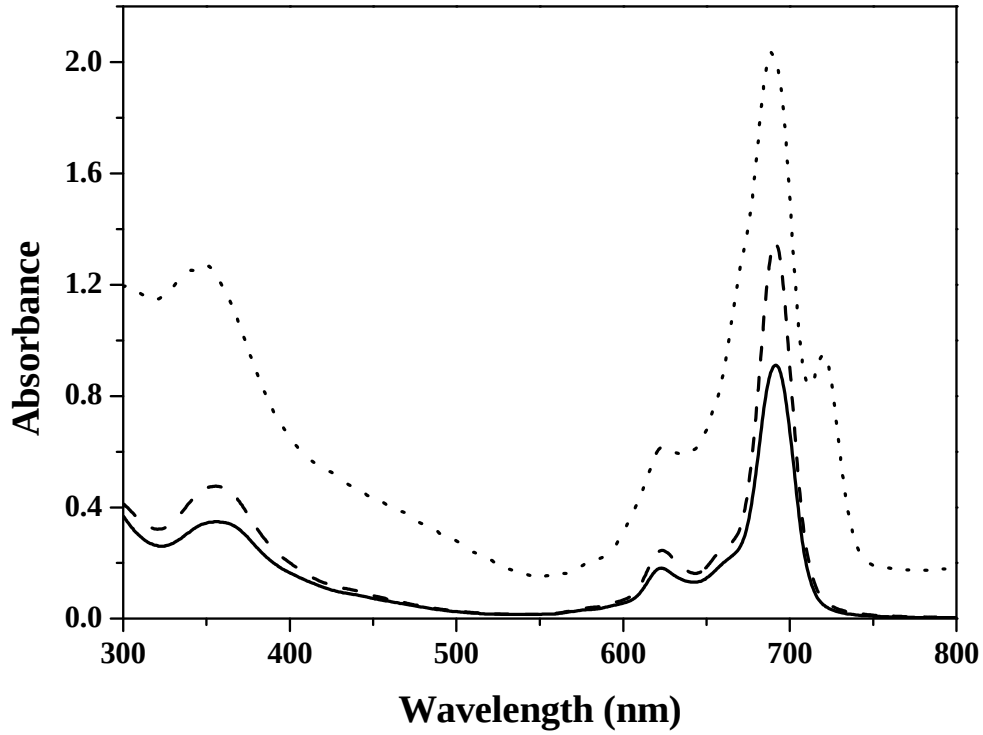

Figure 2

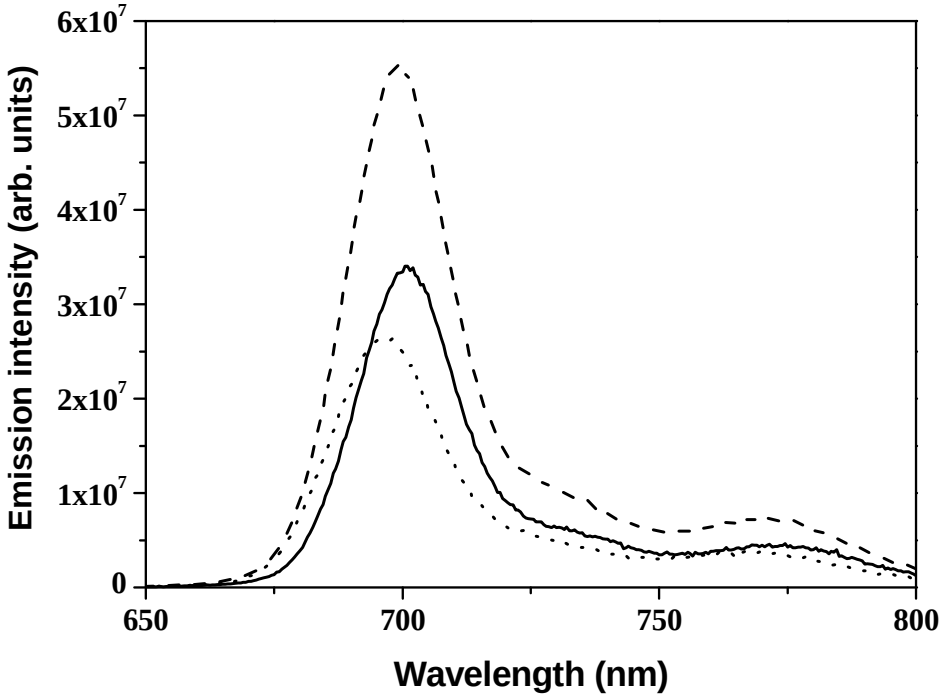
Emission intensity (arb. units)
6x10^7
5x10^7
4x10^7
3x10^7
2x10^7
1x10^7
0
650
700
750
800
Wavelength (nm)

Figure 3

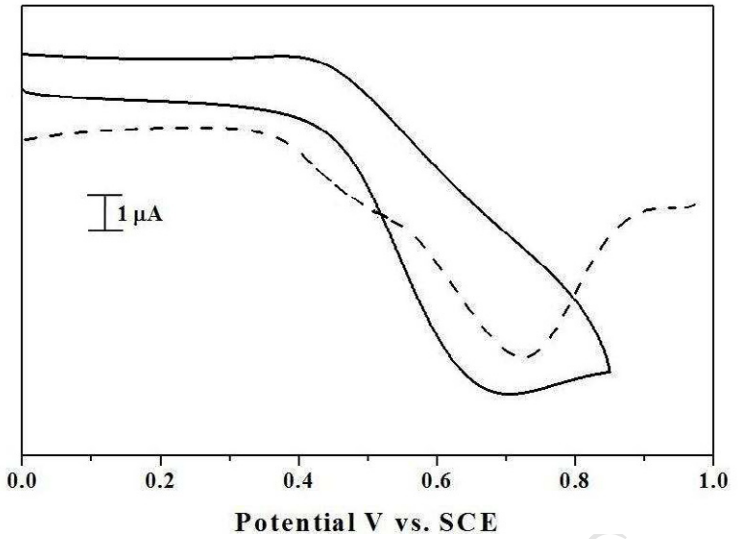
1 µA
0.0
0.2
0.4
0.6
0.8
1.0
Potential V vs. SCE

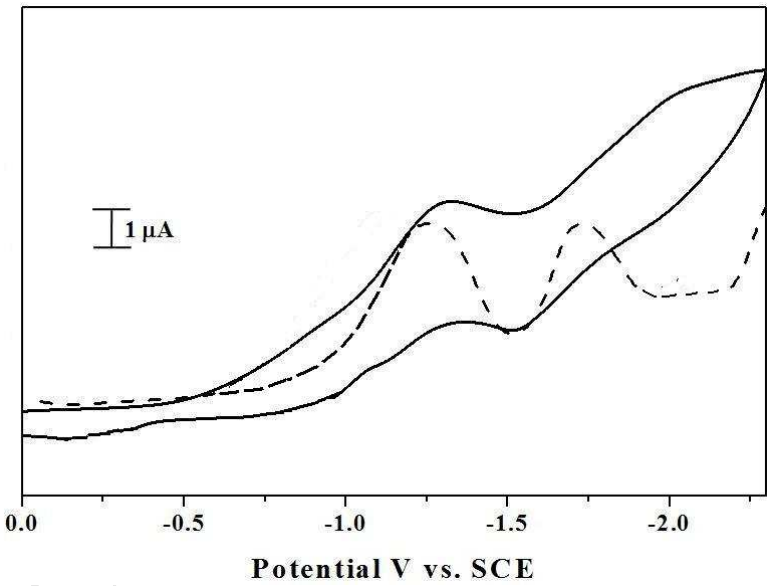
1 µA
0.0
-0.5
-1.0
-1.5
-2.0
Potential V vs. SCE

Figure 4

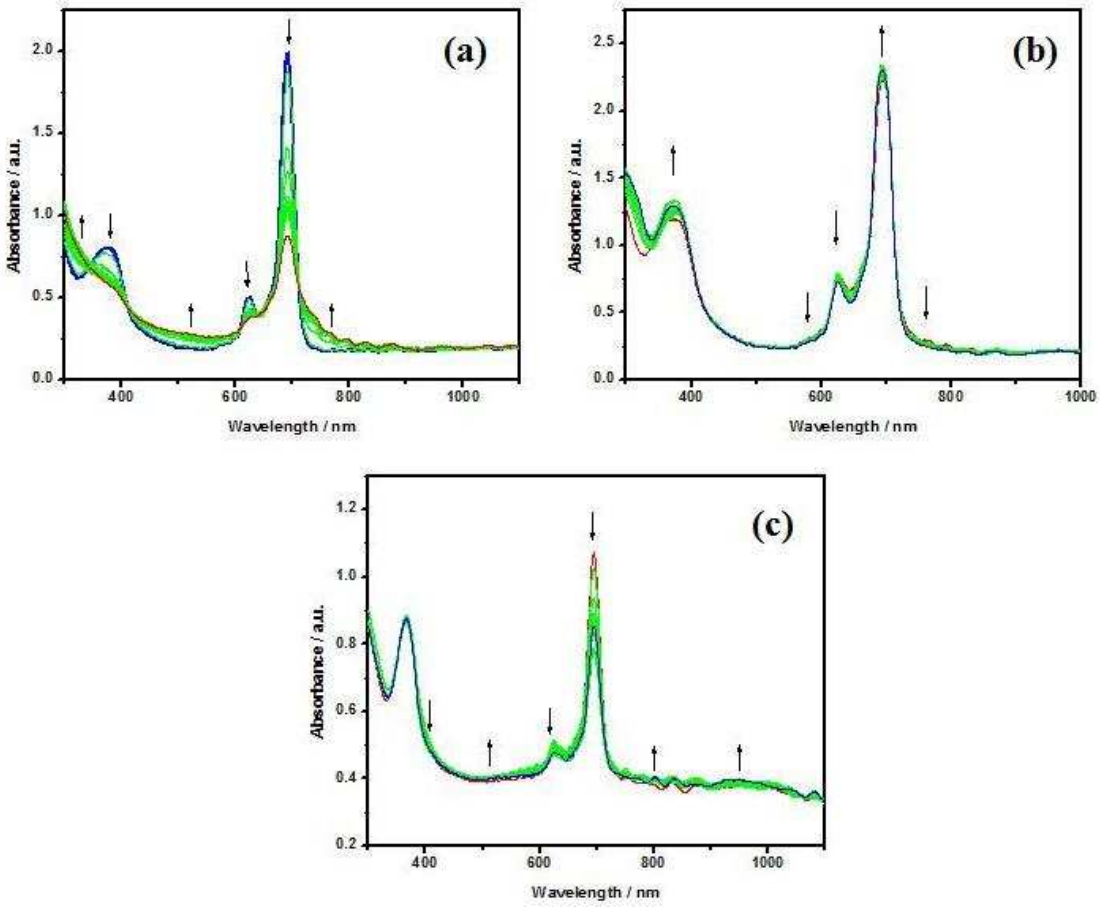
(a)
Absorbance / a.u.
Wavelength / nm
(b)
Absorbance / a.u.
Wavelength / nm
(c)
Absorbance / a.u.
Wavelength / nm

Figure 5

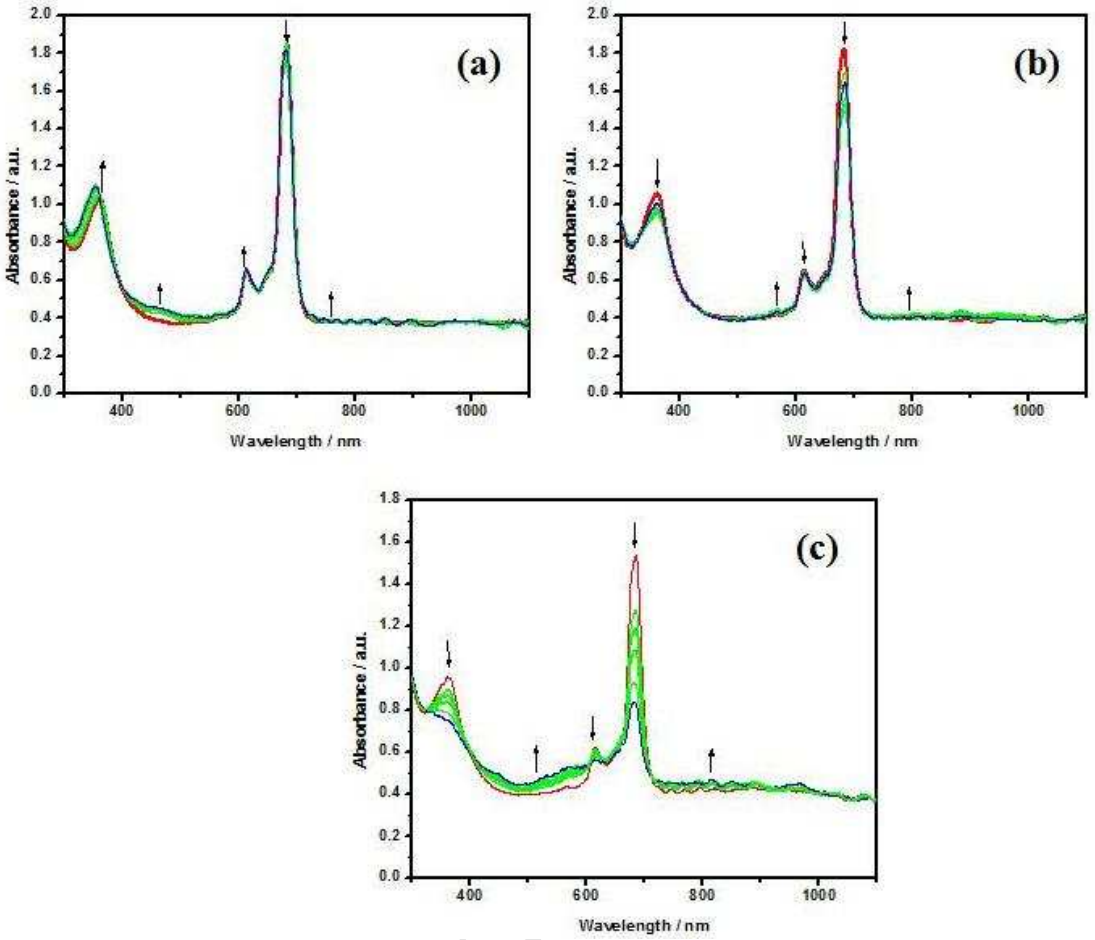

Figure 6

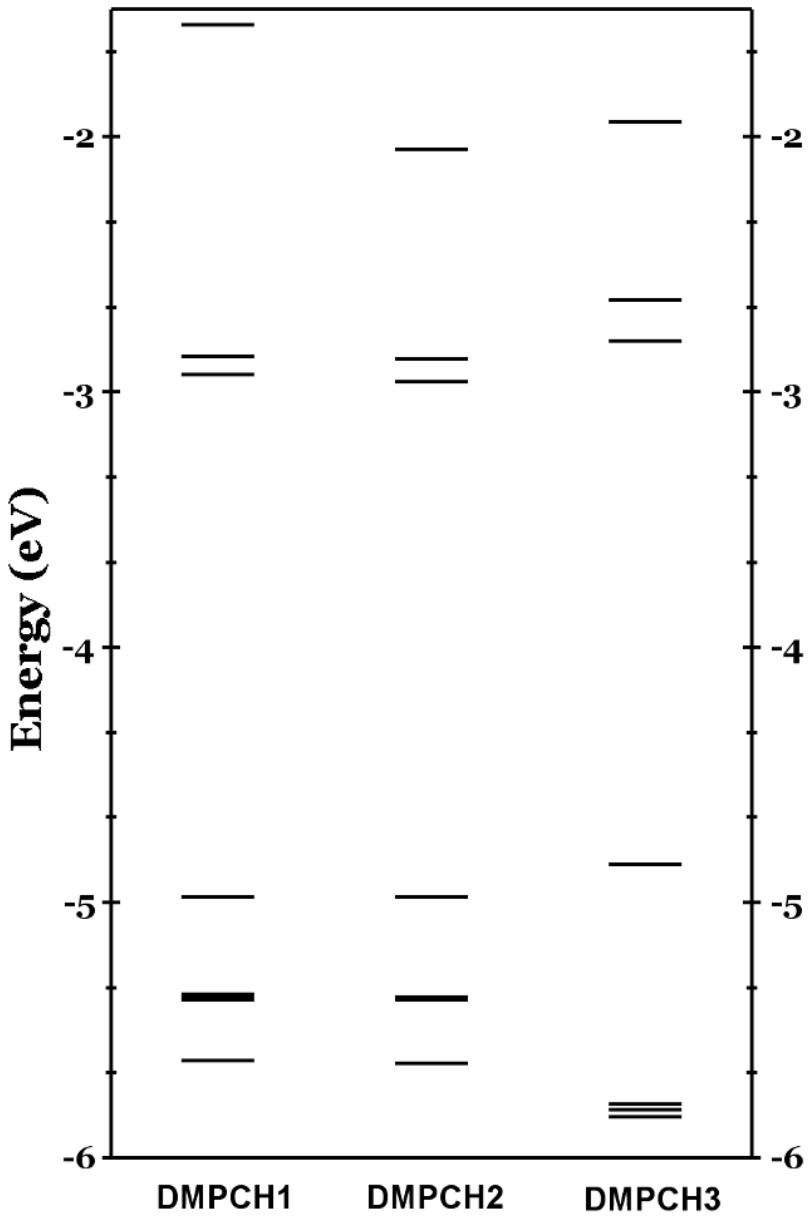

Figure 7

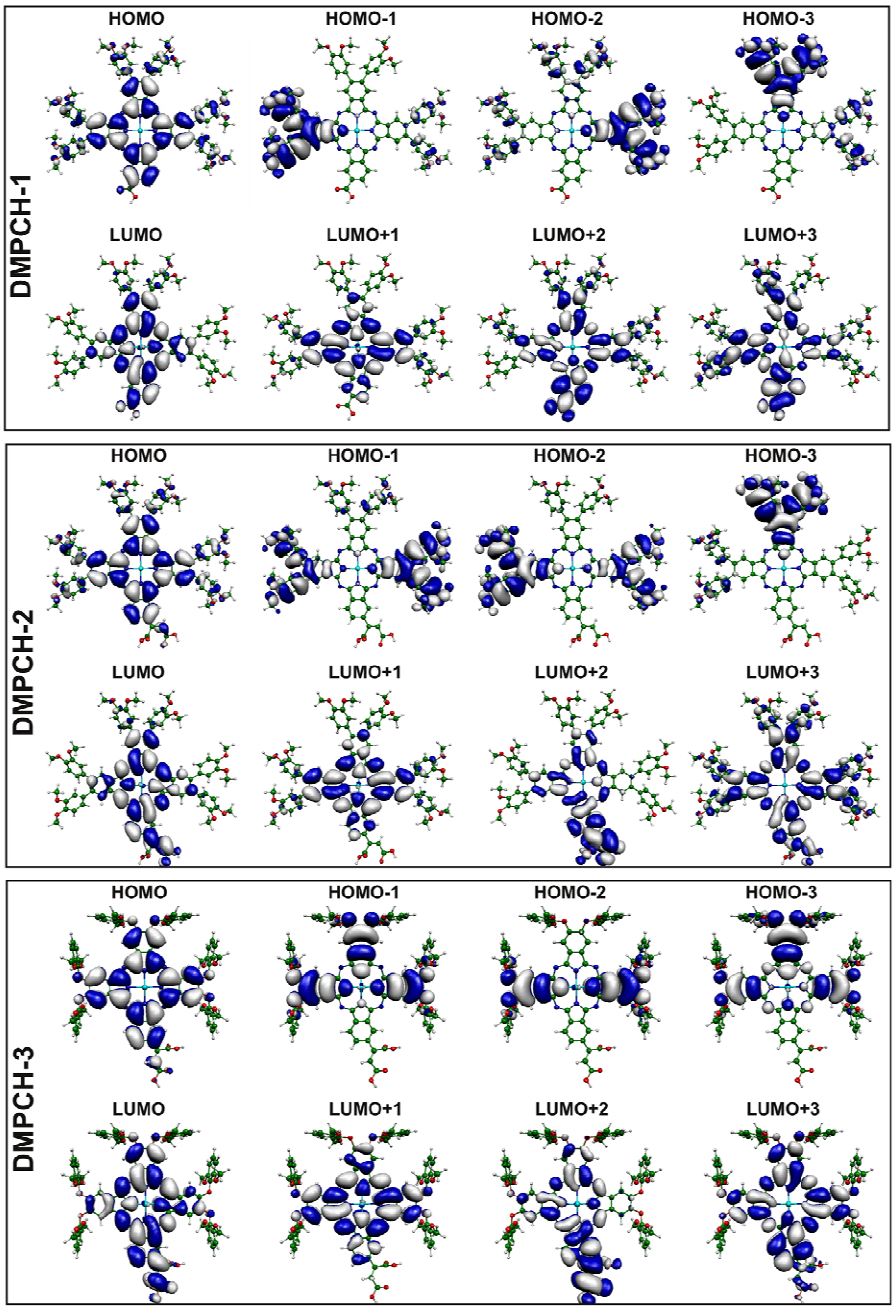
DMPCH-1
HOMO
HOMO-1
HOMO-2
HOMO-3
LUMO
LUMO+1
LUMO+2
LUMO+3
DMPCH-2
HOMO
HOMO-1
HOMO-2
HOMO-3
LUMO
LUMO+1
LUMO+2
LUMO+3
DMPCH-3
HOMO
HOMO-1
HOMO-2
HOMO-3
LUMO
LUMO+1
LUMO+2
LUMO+3

Figure 8

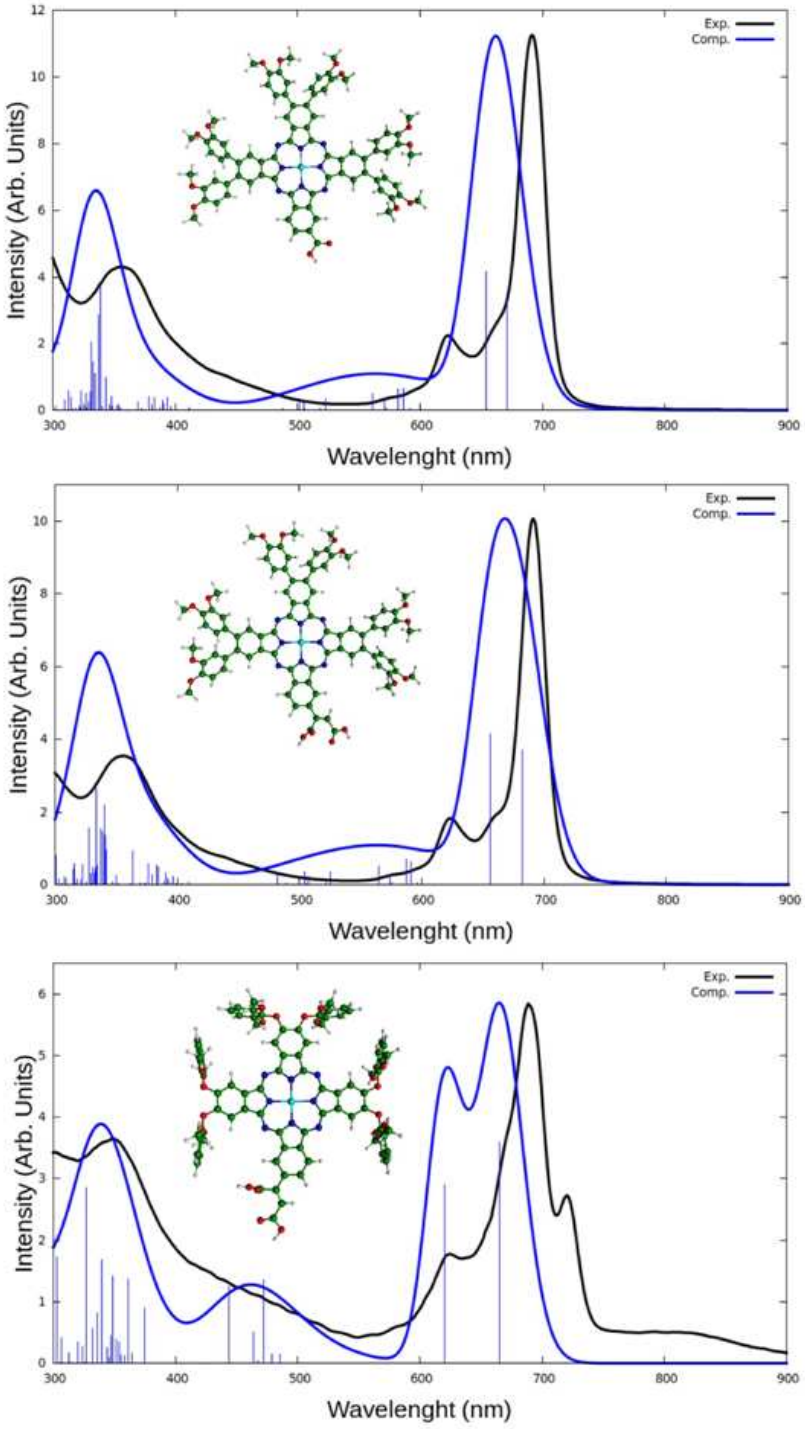
Exp.
Comp.
Intensity (Arb. Units)
Wavelenght (nm)
Exp.
Comp.
Intensity (Arb. Units)
Wavelenght (nm)
Exp.
Comp.
Intensity (Arb. Units)
Wavelenght (nm)

Figure 9

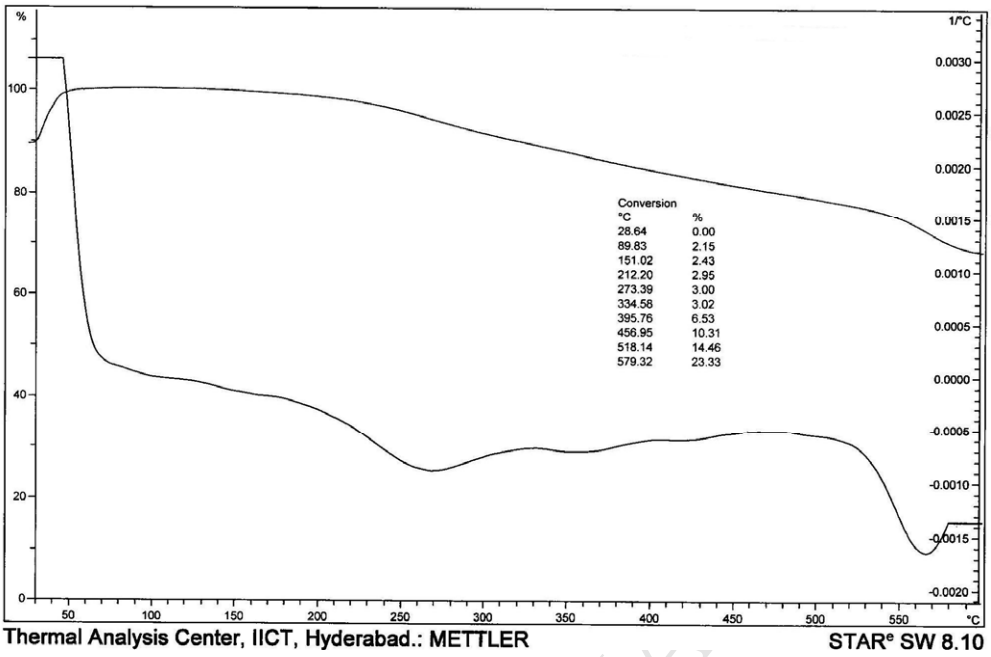
%
1/°C
100
80
60
40
20
0
0.0030
0.0025
0.0020
0.0015
0.0010
0.0005
0.0000
-0.0005
-0.0010
-0.0015
-0.0020
50
100
150
200
250
300
350
400
450
500
550
°C
Conversion
°C %
28.64 0.00
89.83 2.15
151.02 2.43
212.20 2.95
273.39 3.00
334.58 3.02
395.76 6.53
456.95 10.31
518.14 14.46
579.32 23.33
Thermal Analysis Center, IICT, Hyderabad.: METTLER
STAR° SW 8.10

Figure 10

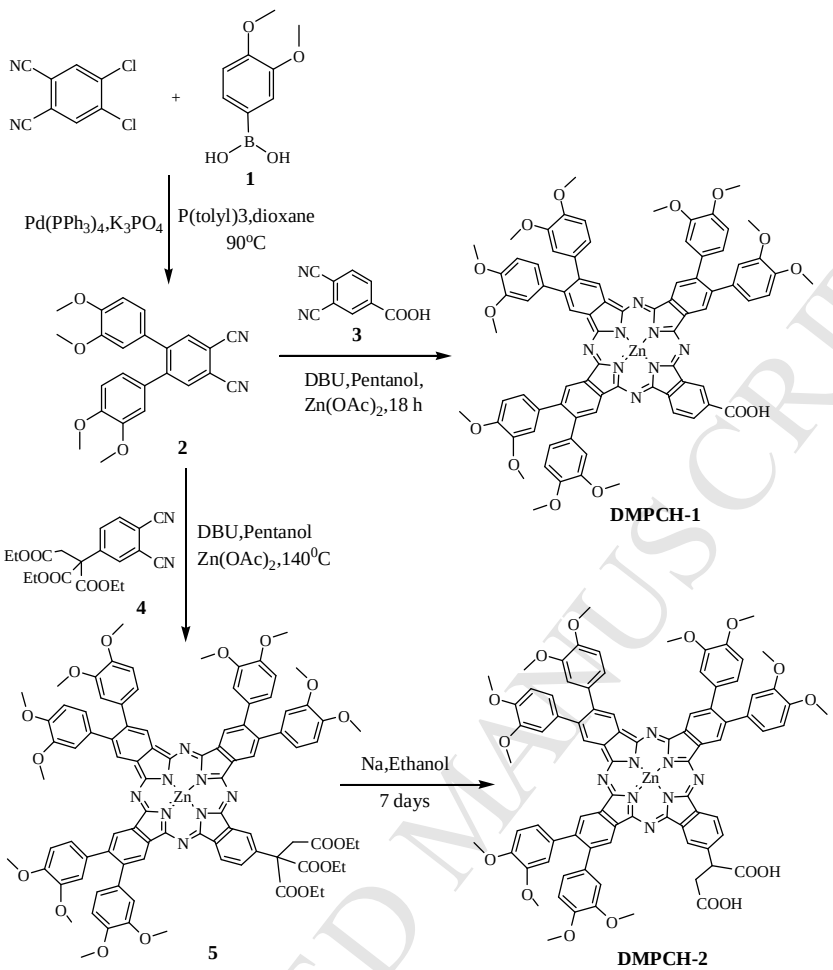

Scheme-1

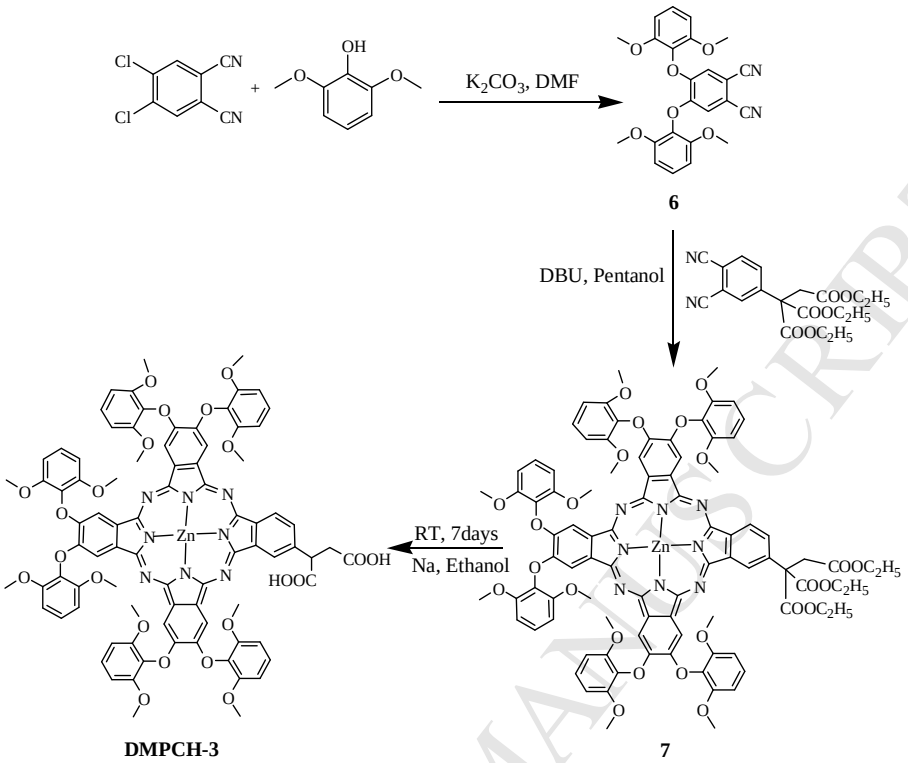

Scheme-2

Sterically Demanded Unsymmetrical Zinc Phthalocyanines for Dye-Sensitized Solar Cells

L. Giribabu,[a] V.K. Singh,[a] Tejaswani Jella,[a] Y. Sounanya,[b] Anna Amat,[c,d] Filippo De Angelis[c] Aswani Yella,[e] Peng Gao,[e] Mohammad Khaja Nazeeruddin[e]

[a] *Inorganic & Physical Chemistry Division, Indian Institute of Chemical Technology, Hyderabad-500607, India.Email: giribabu@iict.res.in*

[b]*Molecular Modelling Group, Indian Institute of Chemical Technology, Hyderabad-500067, India*

[c]*Istituto di Scienzee Tecnologie Molecolari del CNR (CNR-ISTM), Via Elce di Sotto 8, I-06100 Perugia, Italy. Fax: +39-075-585 5606; Tel: +39-075-585 5522/5526*

[d]*Dipartimento di Chimica, Università di Perugia, Via elce di Sotto 8, 06213 Perugia, Italy*

[e]*Laboratory for Photonics and Interfaces, Institute of Chemical Sciences and Engineering, School of basic Sciences, Swiss Federal Institute of Technology, CH - 1015 Lausanne, Switzerland. E-mail:mdkhaja.nazeeruddin@epfl.ch. Tel. +41-21-6936124. Fax: +41-21-6934111.*

^{1}H NMR Spectrum of 2 in $CDCl_3$

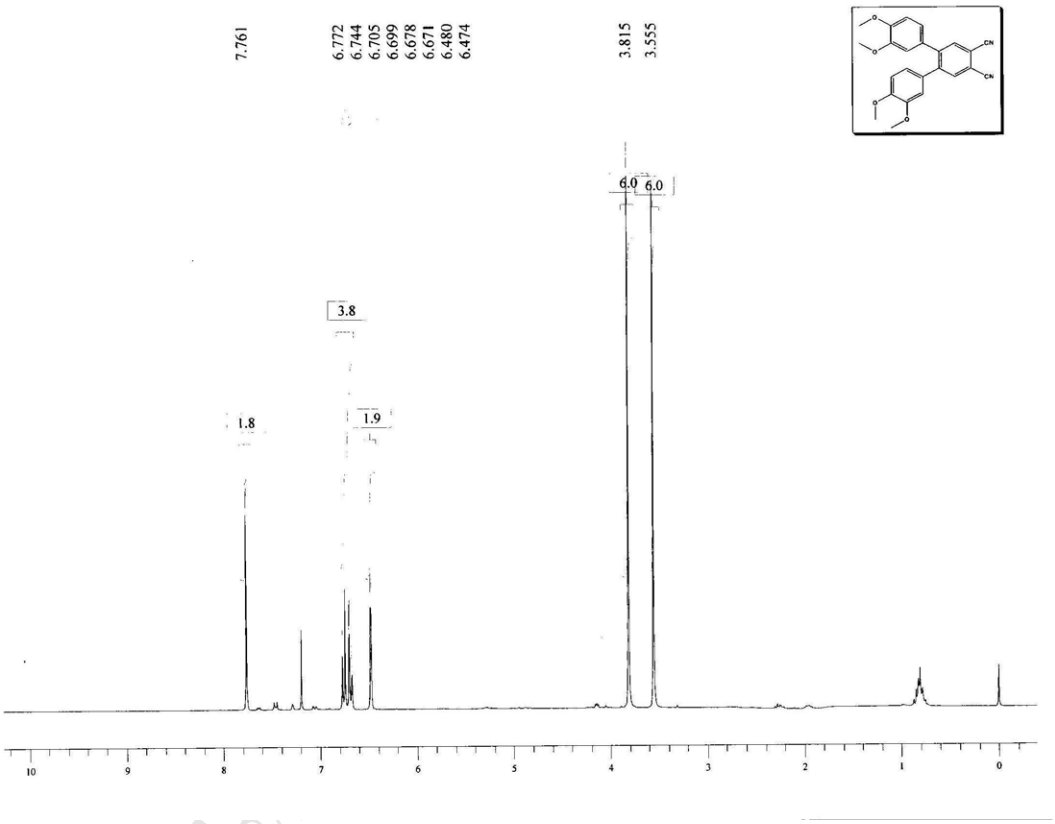

IR Spectrum of 2

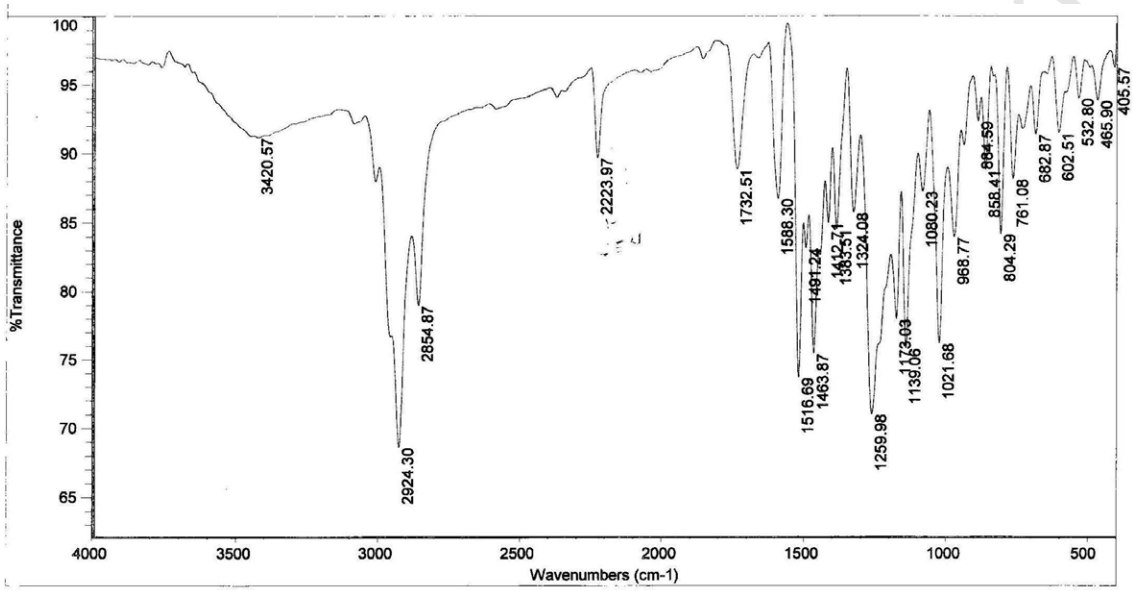

Mass Spectrum of 2

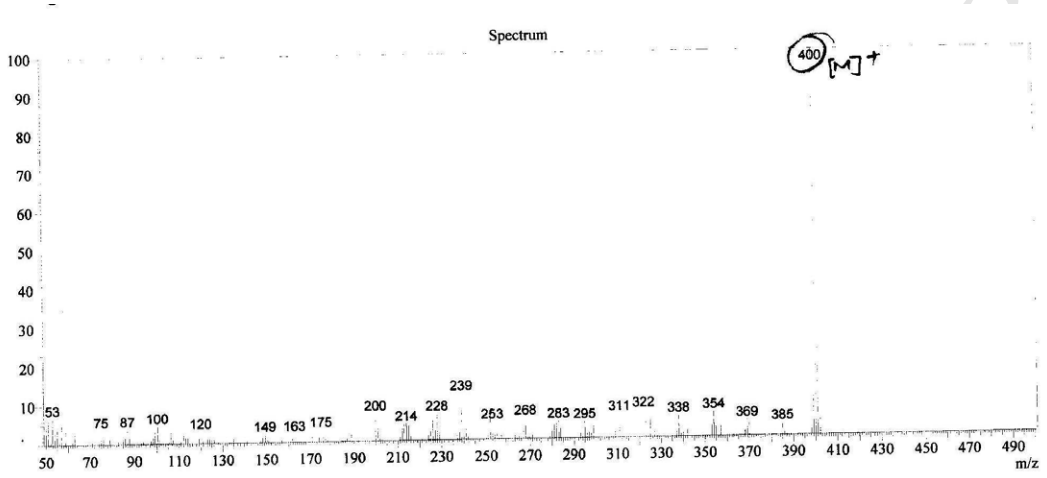

Mass Spectrum of DMPCH-1

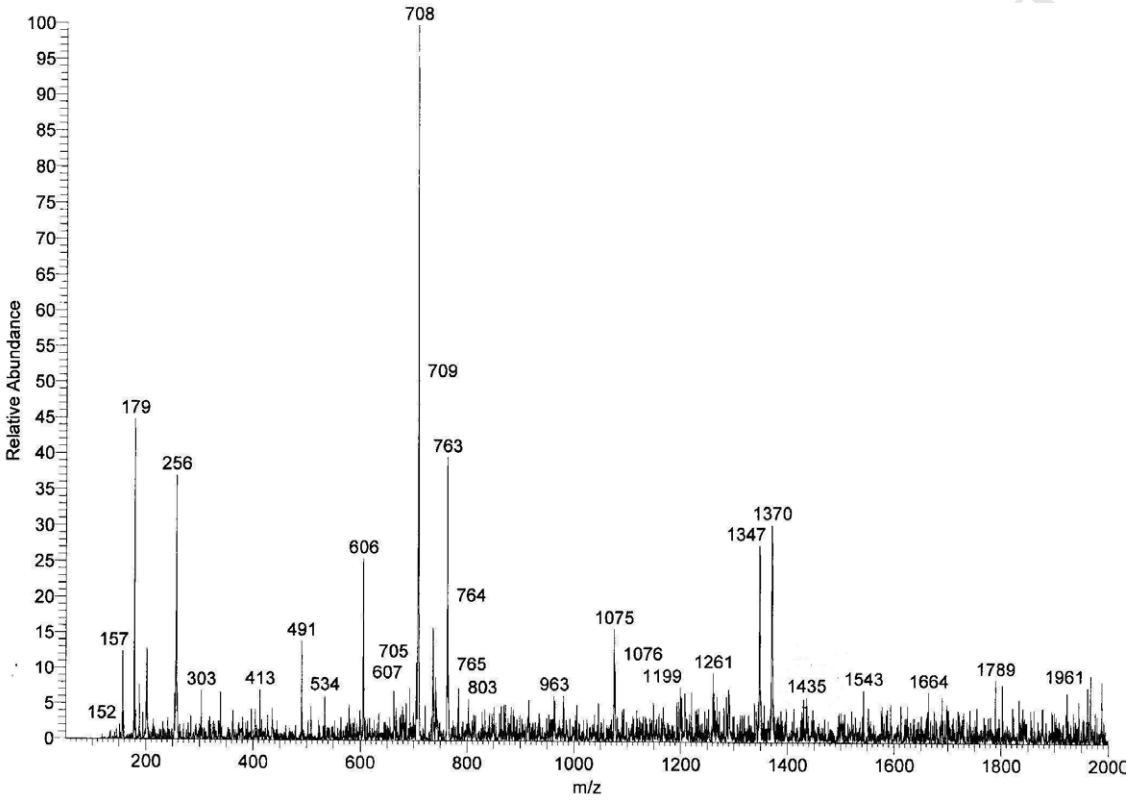

IR Spectrum of DMPCH-1

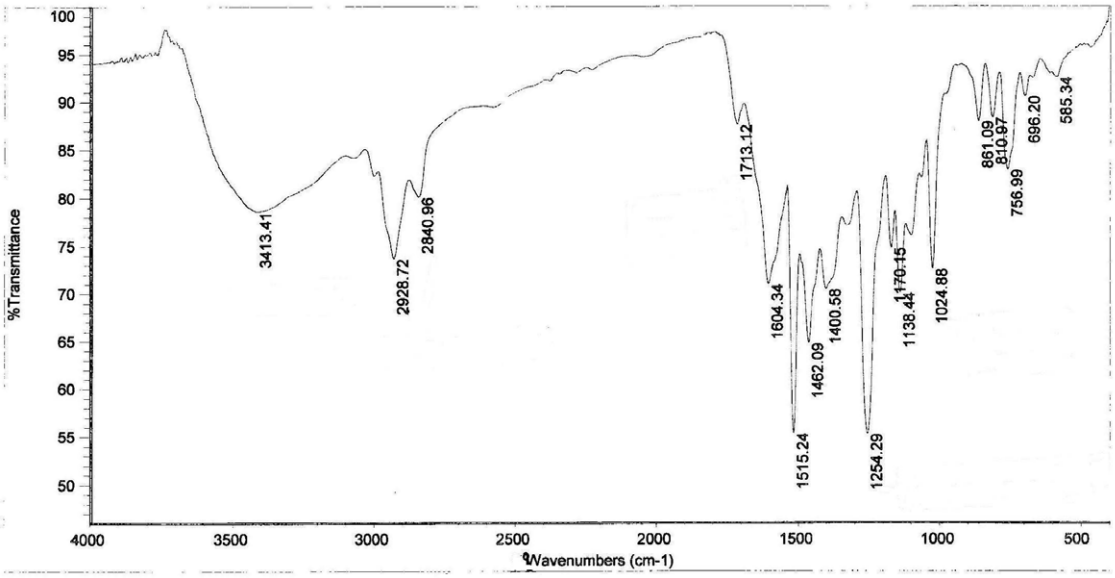

Mass Spectrum of 6

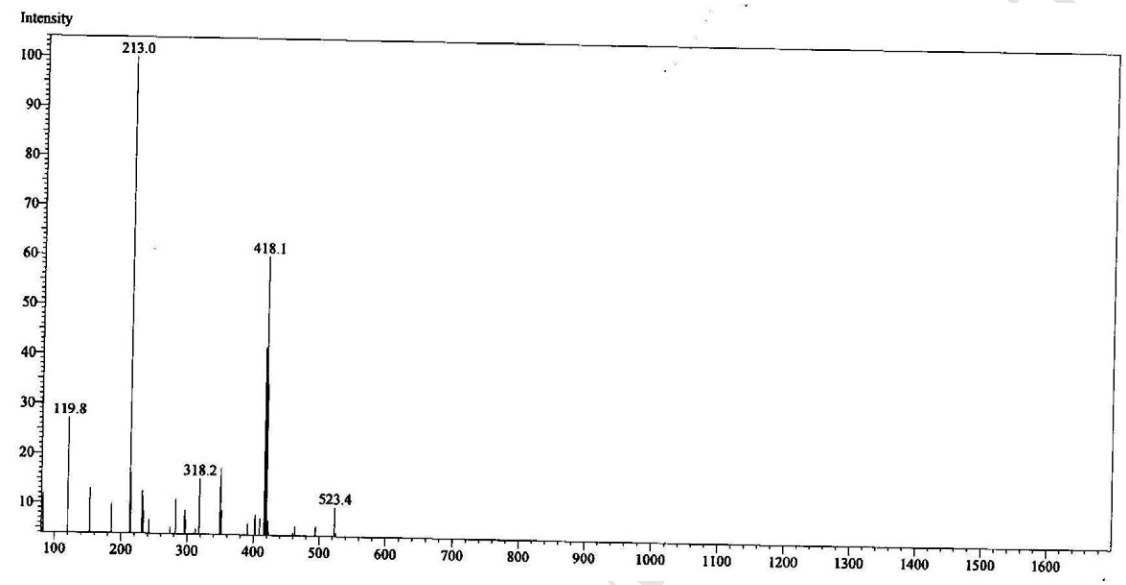

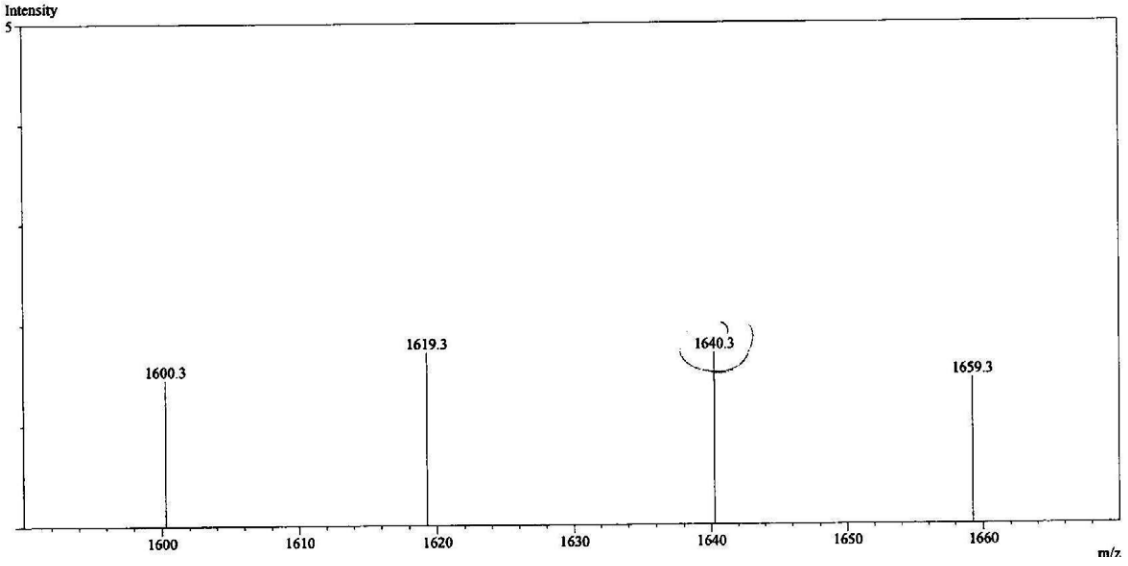

IR Spectrum 6

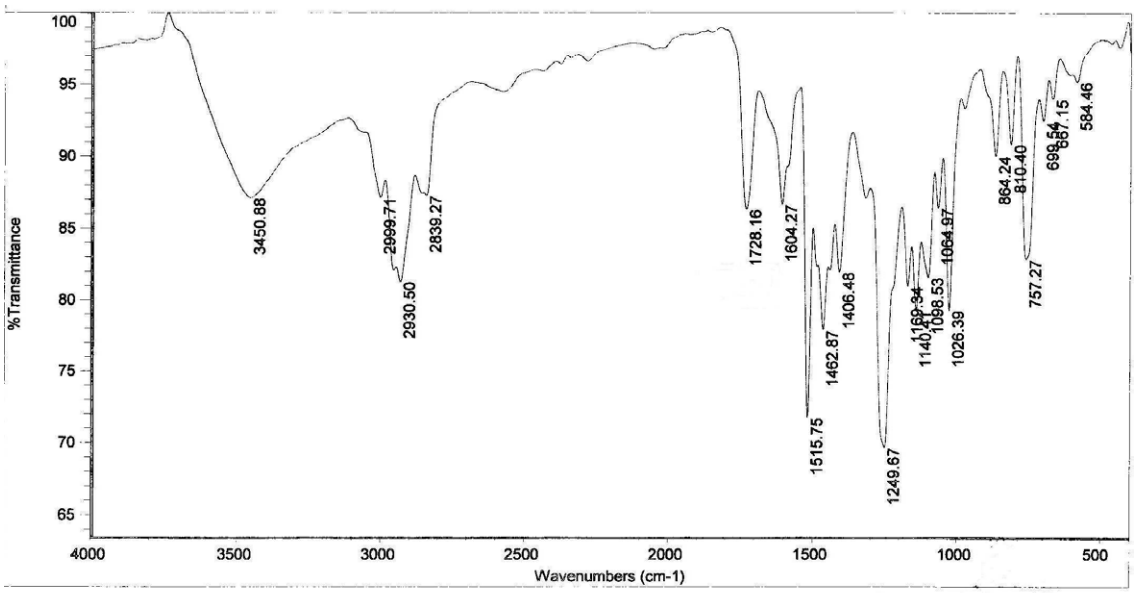

^{1}H NMR Spectrum of 6 in $CDCl_3$

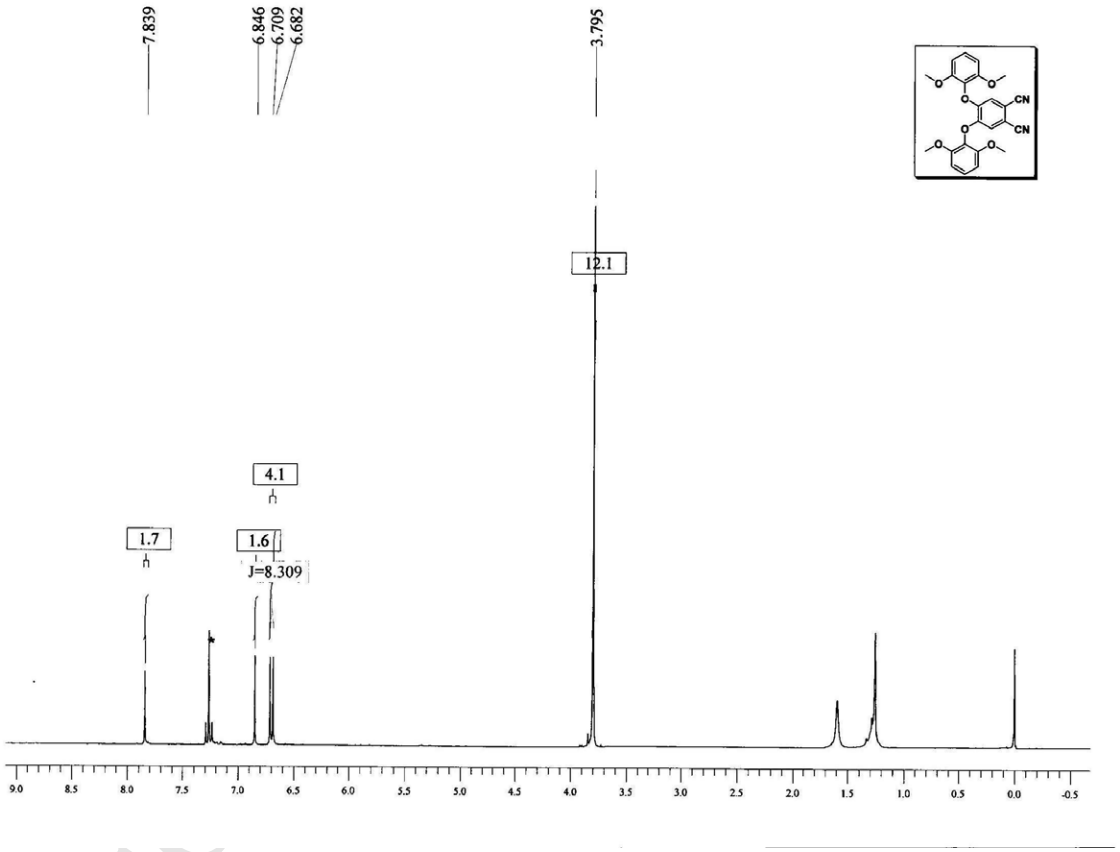

IR Spectrum of 6

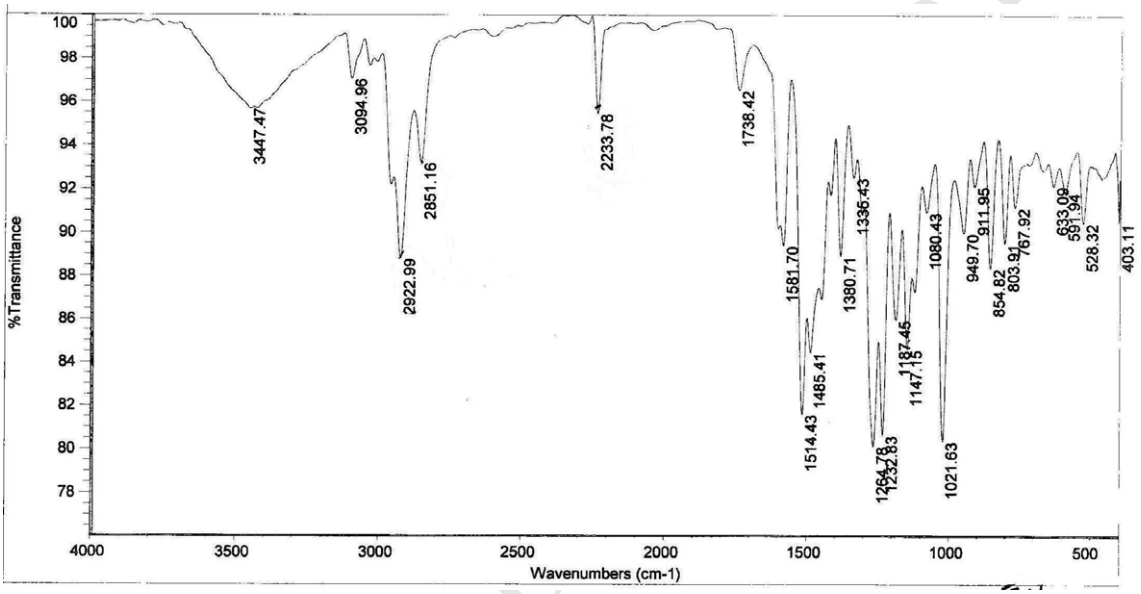

Mass Spectrum of 6

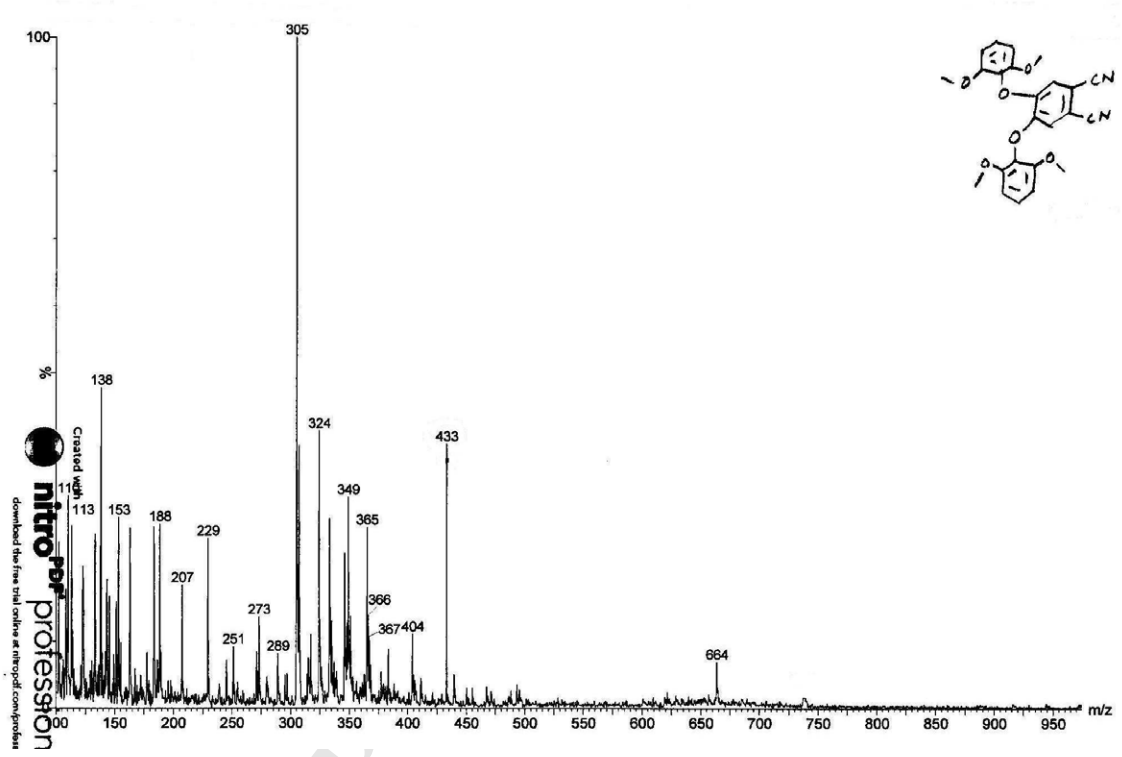

Mass Spectrum of DMPCH-3

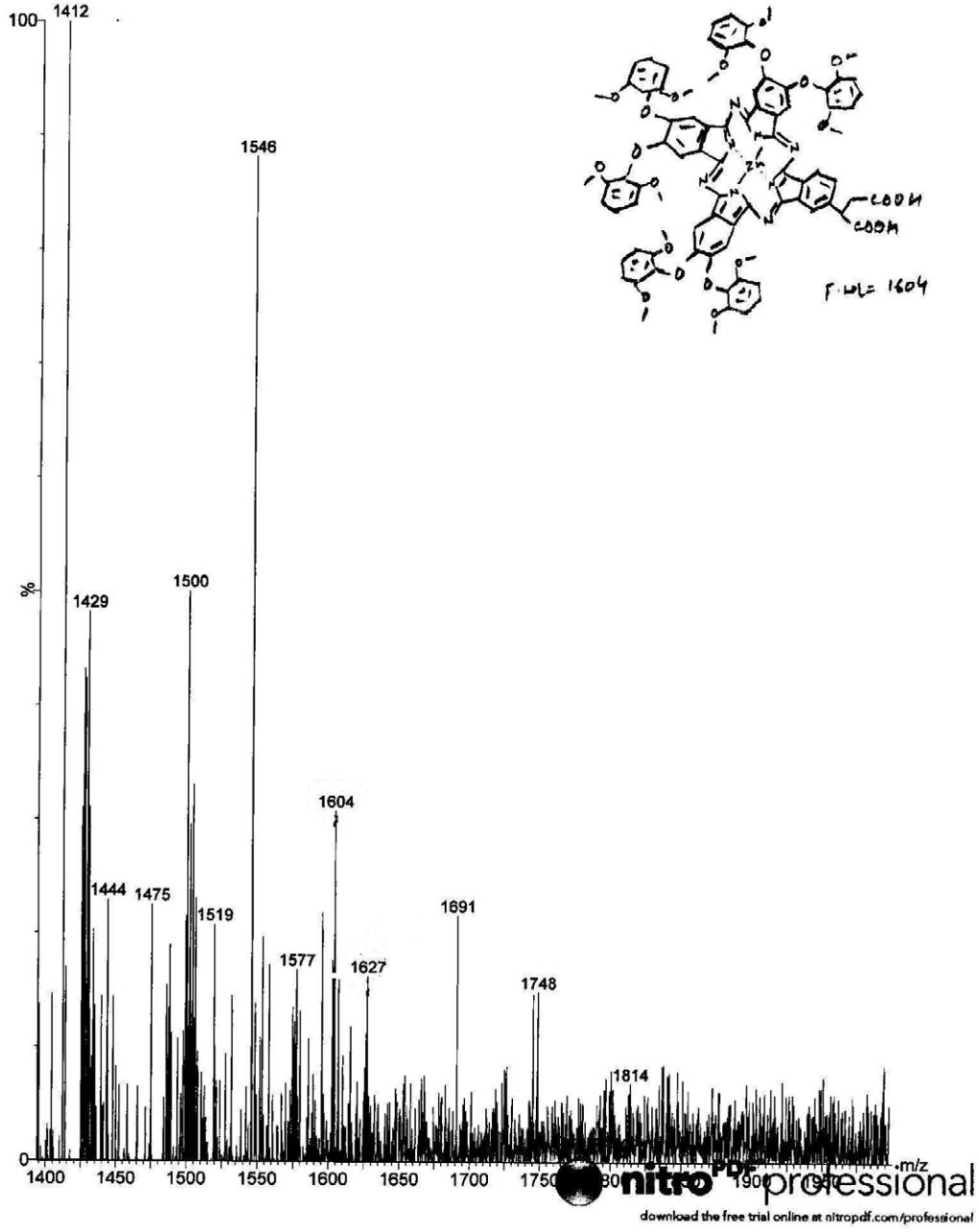

Fluorescence spectra of DMPCH-1 (——) in CH_2Cl_2 and (——)adsorbed onto a 2 μm thick TiO_2 film, DMPCH-2 (——) in CH_2Cl_2 and (——)adsorbed onto a 2 μm thick TiO_2 film, DMPCH-3 (——) in CH_2Cl_2 and (——)adsorbed onto a 2 μm thick TiO_2 film The excitation wavelength λ_{ex} = 700 nm.

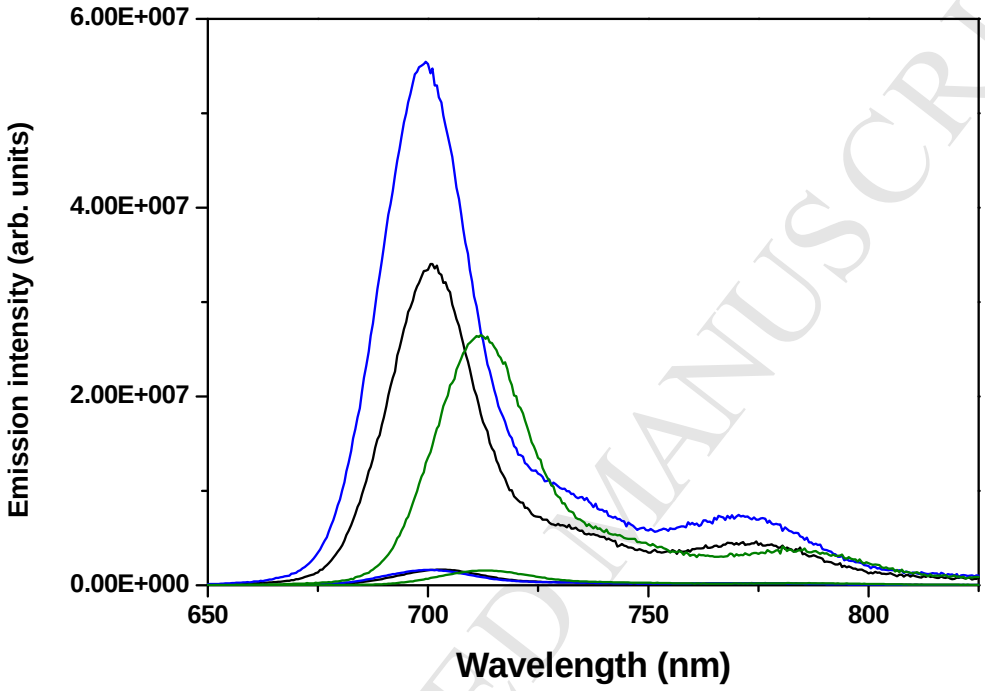

Fluorescence Decay of DMPCH-1 in THF

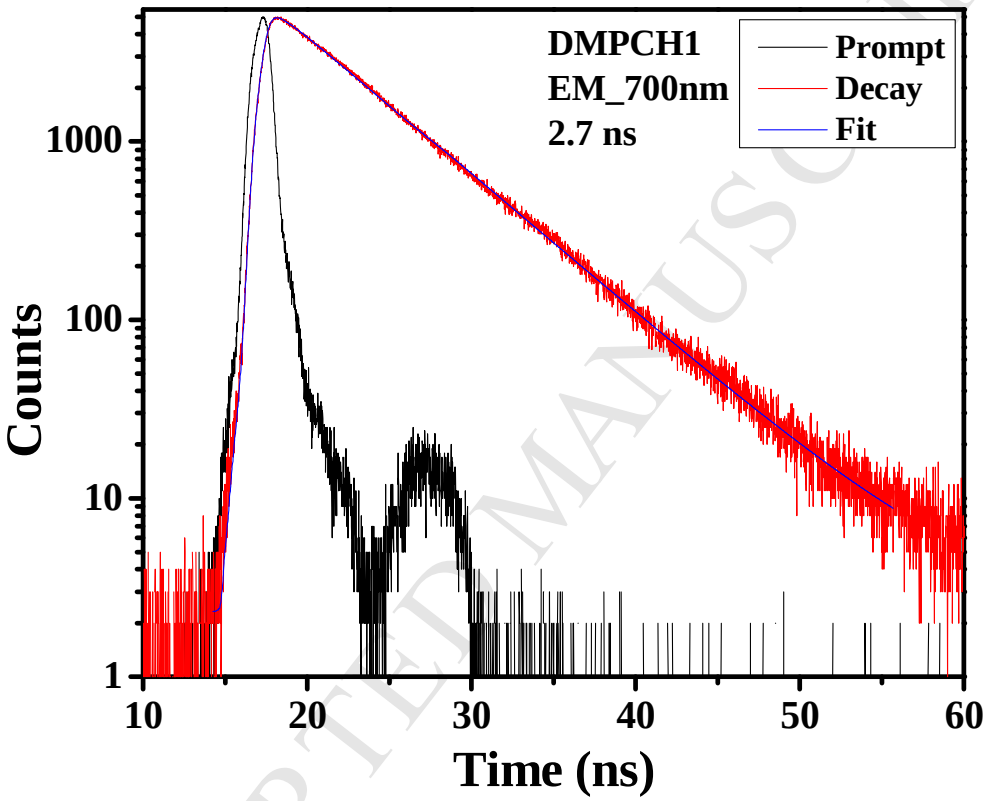

Fluorescence Decay of DMPCH-2 in THF

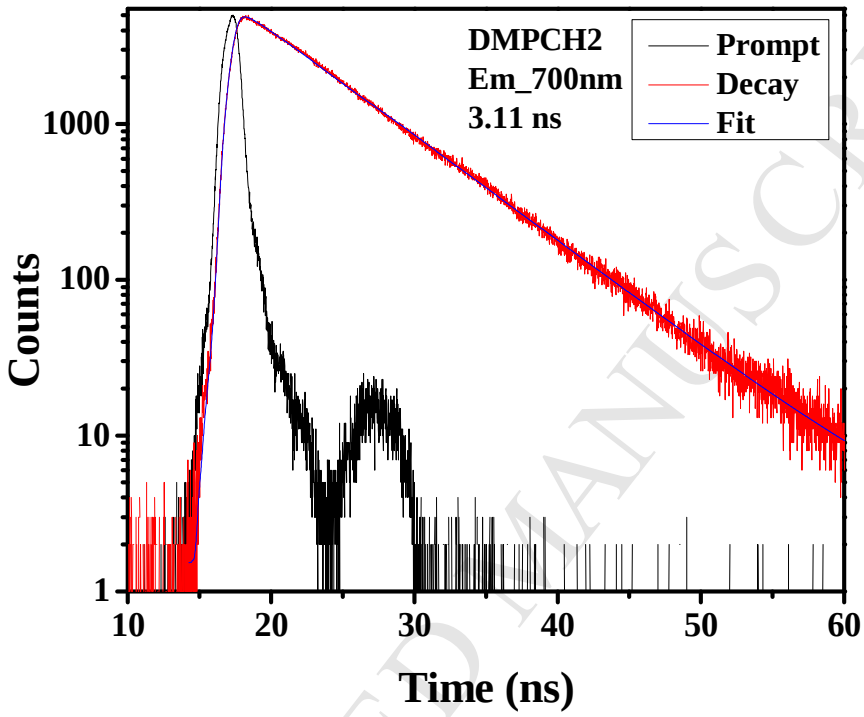

Fluorescence Decay of DMPCH-3 in THF

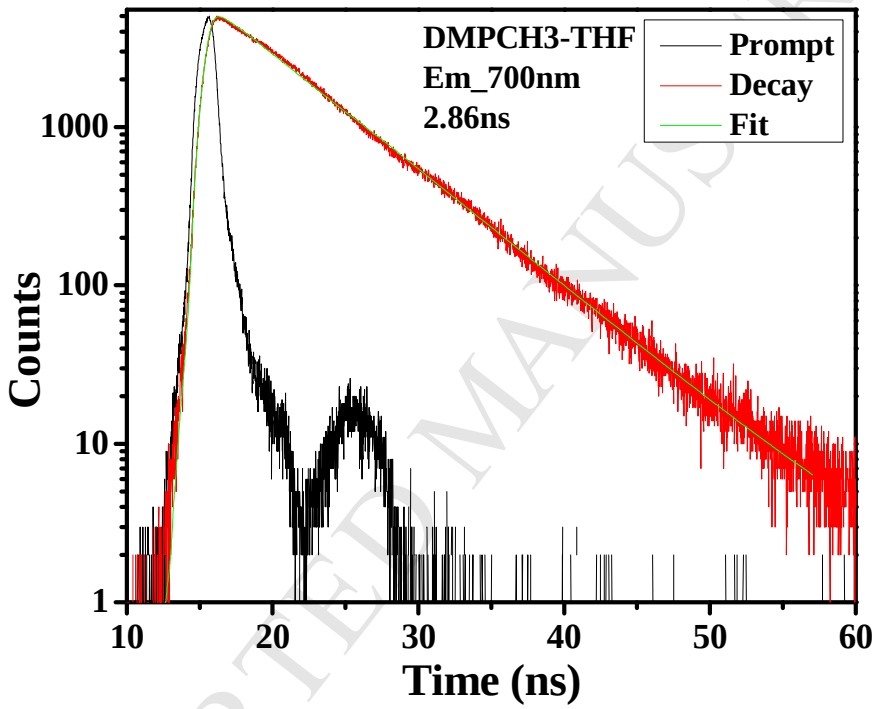

(a) Photocurrent action spectrum of DMPCH-1 and (b) Current-voltage characteristics of DMPCH-1. The redox electrolyte composition is 0.6 M 1,3-dimethylimidazolium iodide, 0.03 M iodine, 0.05 M LiI, 0.05 M guanidinium thiocyanate, and 0.25 M 4-*tert*-butylpyridine in 15/85 (v/v) mixture of valeronitrile and acetonitrile and the cell's active area 0.185 cm^2.

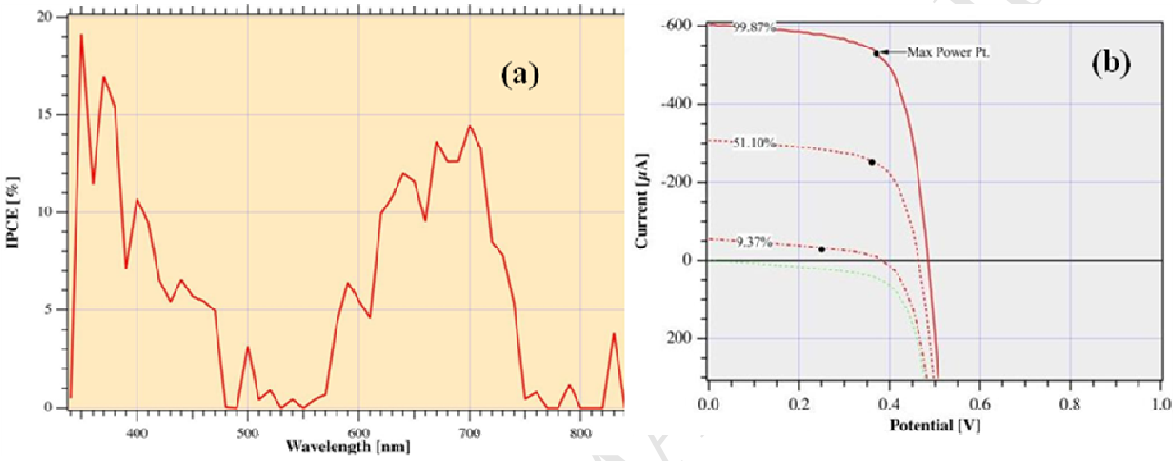

(a) Photocurrent action spectrum of DMPCH-2 and (b) Current-voltage characteristics of DMPCH-2. The redox electrolyte composition is 0.6 M 1,3-dimethylimidazolium iodide, 0.03 M iodine, 0.05 M LiI, 0.05 M guanidinium thiocyanate, and 0.25 M 4-*tert*-butylpyridine in 15/85 (v/v) mixture of valeronitrile and acetonitrile and the cell's active area 0.185 cm^2.

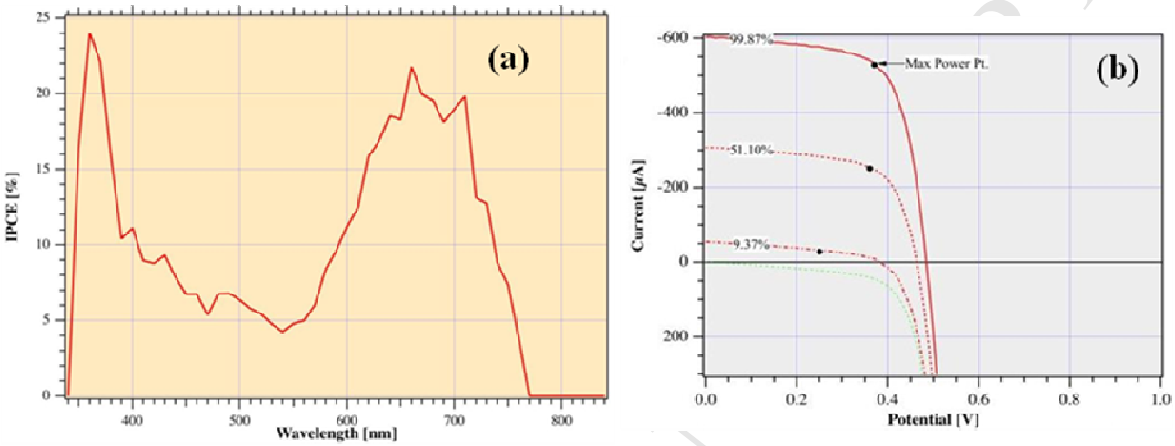

Current-voltage characteristics of DMPCH-3

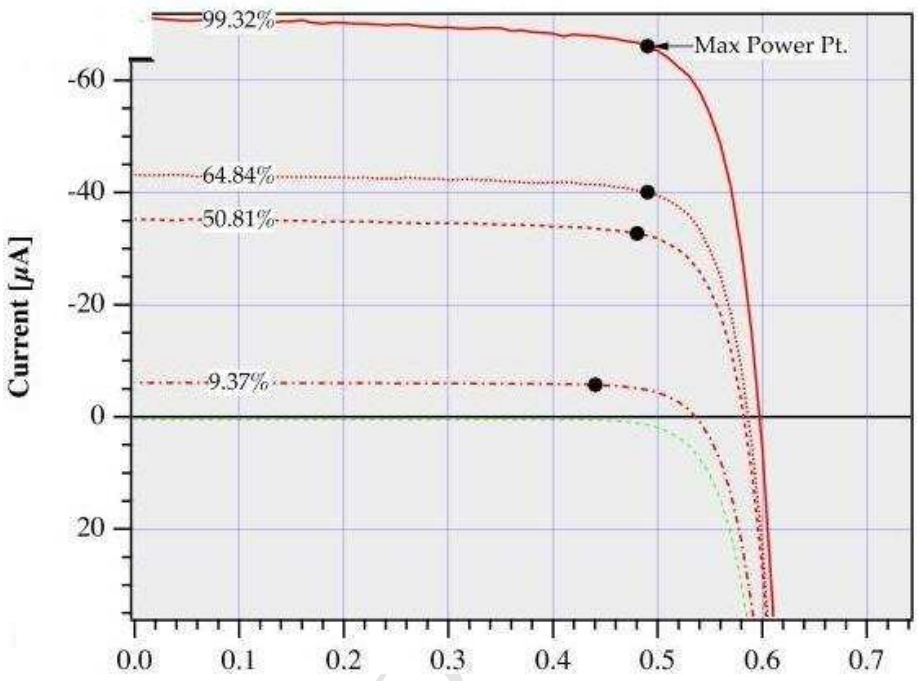

TG/DTG curves of DMPCH-2 with heating rate of 10 ^{o}C min^{-1} under nitrogen.

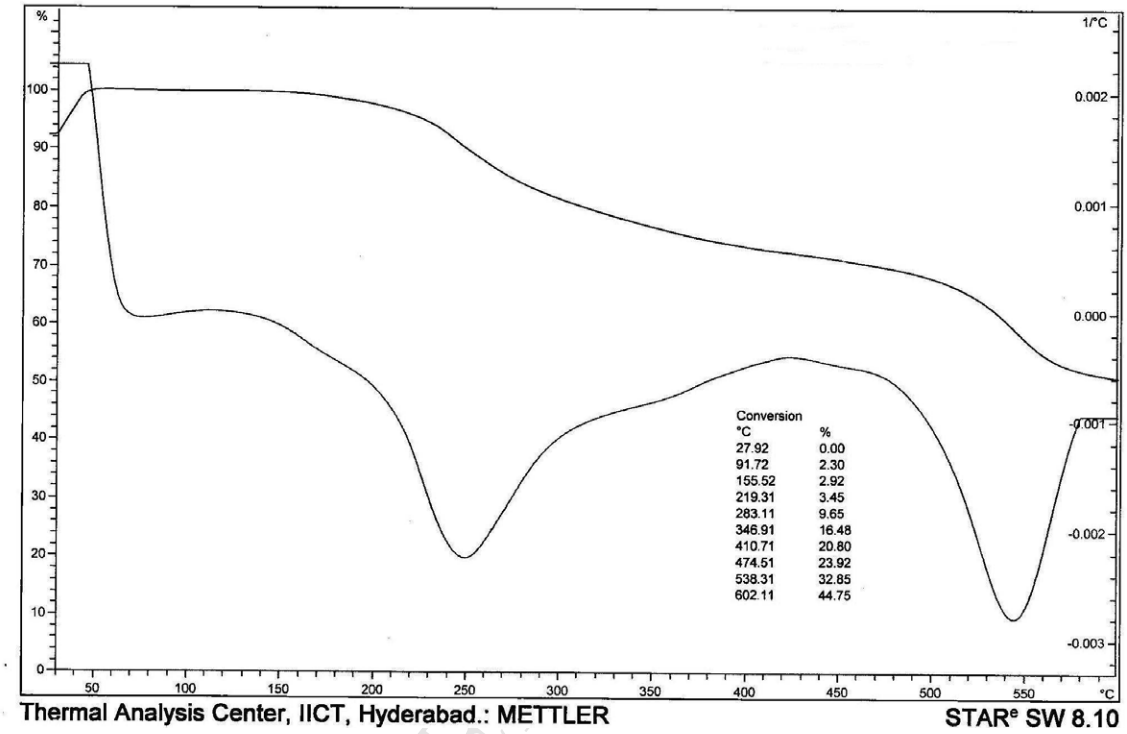

TG/DTG curves of DMPCH-3 with heating rate of 10 ^{o}C min^{-1} under nitrogen.